Abdominal Radiology (2019) 44:3408–3431
https://doi.org/10.1007/s00261-019-02200-2

REVIEW

Incidental fetal imaging with CT: a pictorial essay

Kelly Tornow[1] · Kristen Bishop[1] · Travis Browning[1]

Published online: 5 September 2019

Abstract
Although CT is not the first choice for abdominal imaging of pregnant patients, it can be indicated for pregnant patients with emergent life-threatening conditions. It is prudent in these cases for the radiologist to be familiar with the normal appearance of the pregnant uterus on CT and to evaluate the female pelvis for potential maternal and fetal abnormalities. We aim to provide examples of the normal CT appearance of the female pelvis related to different gestational ages and to demonstrate variant and abnormal conditions of pregnancy which may be identified by CT.

Keywords Humans · Female · Pregnancy · Fetus · Uterus · Pelvis · Tomography, X-ray computed

Introduction

Imaging modalities utilizing ionizing radiation such as CT are typically avoided during pregnancy to protect the fetus from potential adverse effects of radiation. In specific situations, however, emergent CT is needed to evaluate maternal health, as a delay in diagnosis can be life-threatening to both the mother and fetus, and depending on gestational age of the fetus, imminent maternal demise will affect fetal viability [1]. The current American College of Obstetricians and Gynecologists guidelines recommend against withholding CT from pregnant patients when ultrasound or MRI is not a reasonable alternative [2]. In addition, the practice parameters from the American College of Radiology and the Society for Pediatric Radiology state that although there is no safe level of radiation exposure, the radiation dose to the conceptus from a single CT scan is well below any threshold dose necessary to induce developmental abnormalities (50 mGy) [3]. In emergent clinical settings, the CT imaging of the fetus is incidental and not the intent of the exam. However, the fetus is included in the field of view and should not be excluded from the image review process. The purpose of this pictorial essay is to review the normal CT appearance of the pregnant uterus at different gestational ages and provide examples of both normal and abnormal findings.

Normal pregnancy

First trimester

The CT appearance of early pregnancy parallels known developmental processes. The earliest visible findings on CT are subtle, initially presenting as nonspecific endometrial heterogeneity (Fig. 1). Although CT is not diagnostic for early pregnancy, additional extrauterine findings may support the diagnosis, such as an ovarian corpus luteal cyst which is usually present from 5 to 8 weeks gestation [4]. Subsequently, a fluid filled gestational sac may be demonstrated within the endometrial cavity, a finding first seen on ultrasound at roughly 5 weeks gestation (Fig. 2) [5]. Later, the early trophoblast can manifest as curvilinear enhancement in the early placenta (Fig. 3). Subtle but increasingly dense soft tissue fetal pole develops within the gestational sac, but fetal parts are not usually visualized by CT until at least the end of the first trimester [4]. It is important to note that the absence of these findings cannot be used to assess gestational age or potential viability. Standard sonographic assessment should be performed for evaluation of the pregnancy and biometric gestational age determination [5].

✉ Kristen Bishop
Kristen.bishop@utsouthwestern.edu

[1] Department of Radiology, University of Texas Southwestern, 5323 Harry Hines Blvd., Dallas, TX 75390-9178, USA

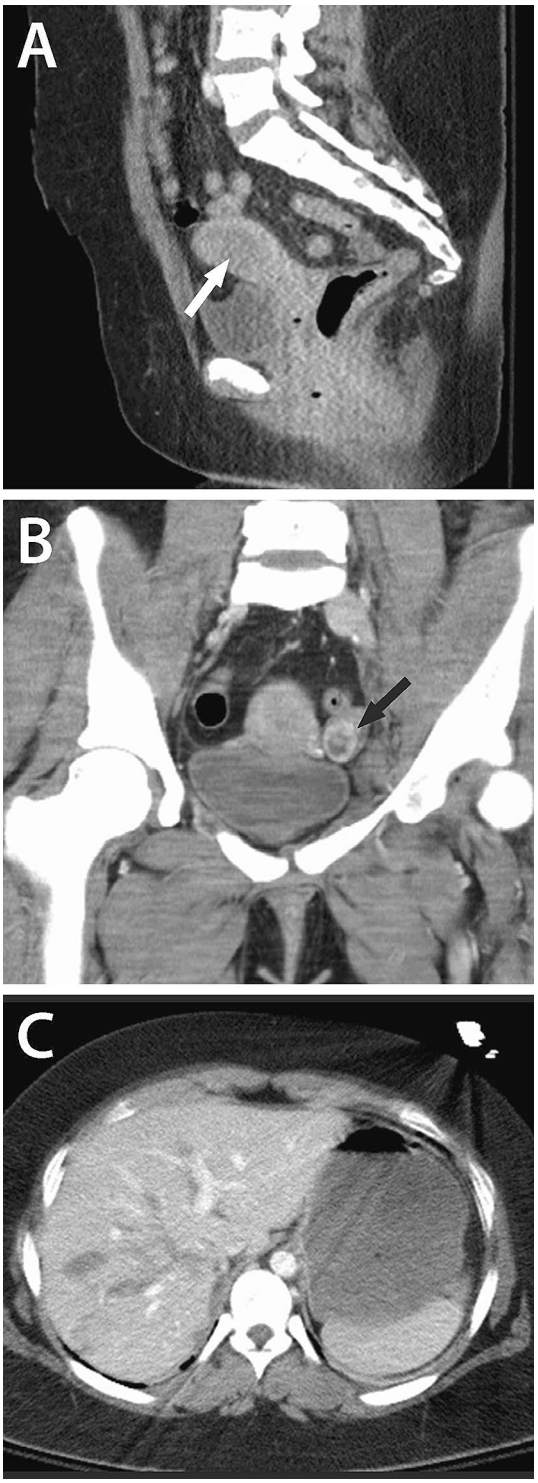

Fig. 1 First trimester pregnancy at estimated gestational age 5 weeks (confirmed on ultrasound). CT images through the pelvis on a scan performed for maternal trauma showing nonspecific signs of early pregnancy such as ill-defined, heterogeneous endometrium (white arrow, **a**) and corpus luteum cyst in the left ovary (black arrow, **b**). Fetal outcome was normal. Maternal hepatic lacerations are also shown (**c**)

Second and third trimester

Fetus

As the pregnancy progresses, the fetal pole becomes progressively dense and more readily identified on CT (Figs. 4, 5). At around 14 weeks gestation, bone mineralization can be identified as increased density on CT (Figs. 6, 7). The mineralization aids in identifying fetal limbs, spine, and skull (Fig. 8). The appropriate degree of mineralization based on gestational age has not been standardized. In our experience, fetal tissues can enhance at a later timing than maternal issues and should not be used to diagnose fetal vascular insult (Fig. 9). With further fetal development, internal soft tissue structures can begin to be distinguished from surrounding fluid (Fig. 10) although structures may be suboptimally evaluated compared to ultrasound and MRI due to lower degree of soft tissue contrast. Ultimately, specific internal organs may be identified in third trimester with progressive development of visible fat primarily in the subcutaneous regions (Figs. 11, 12). In late gestation, we have been able to visualize subtler tissues including the umbilical cord surrounded by amniotic fluid, cord insertion site, and skull sutures, although standard expectations of findings based on fetal development and gestational age have not been developed for CT, and suspected abnormalities can be confirmed with ultrasound (Figs. 13, 14). If delivery is anticipated, fetal position (breach, prone, transverse) can be assessed.

Placenta

The placenta also enlarges and matures over time. Although the placenta is not reliably identified on CT in the first trimester, increased enhancement of the trophoblast can sometimes be seen and becomes more readily apparent beginning in the second trimester (Figs. 3, 4) [6]. The placental attachment can be identified as a hypodense crescent (Fig. 5), which may correspond with the retroplacental clear space described on ultrasound [7, 8]. Placental position (anterior or posterior) and relationship in position to the internal cervical os can be assessed. As the placenta matures, it becomes progressively heterogeneous (Figs. 6, 13, 14). In later gestations, the cotyledons may be identified as rounded areas of hypoenhancement distinct from the enhancing background placenta, similar to their ultrasound appearance (Figs. 11, 13). Venous lakes and placental cysts are also commonly seen hypodensities of the placenta (Figs. 6, 10) [7, 8]. Focal myometrial contractions can artificially cause a thickened appearance of the placenta on CT just as on ultrasound, although real-time monitoring on ultrasound can be used to differentiate (Fig. 9) [6–8].

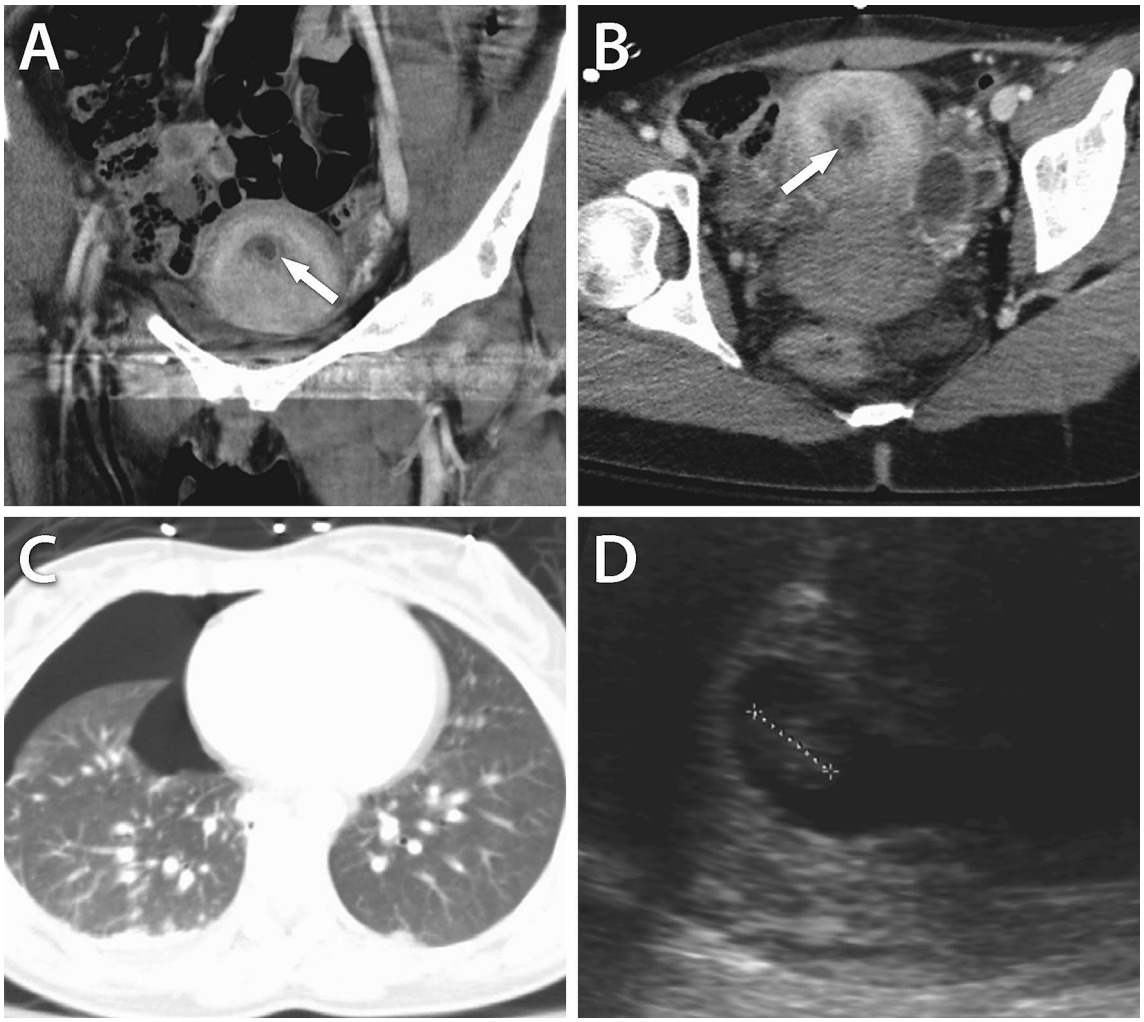

Fig. 2 First trimester pregnancy at estimated gestational age 6 weeks, 4 days. CT images through the pelvis on a scan performed for maternal trauma showing an early gestational sac within the endometrium (white arrows, **a**, **b**). Maternal pneumothorax also shown (**c**). Crown rump length measured on ultrasound 1 week later (**d**), providing estimated gestational age. Fetal outcome was normal

Multiple gestations

Twin gestations occur in up to 3.2% of all pregnancies [9] and can be visualized on CT scan. As with a singleton gestation early in pregnancy, the fetal pole can be identified as subtle soft tissue within a gestational sac, although multiple fetal poles are seen with multiple gestations (Figs. 15, 16). In later pregnancy, distinct fetal skeletons begin to mineralize. Invagination of the chorion between the amniotic membranes in dichorionic diamniotic twin pregnancy correlates with the "twin peak sign" on ultrasound [8].

Abnormal findings of pregnancy

Uterine leiomyomas

Uterine fibroids are benign smooth muscle lesions that affect 20% to 60% of women of childbearing age. Fibroids typically stay stable in size during pregnancy although a small portion has been shown to enlarge during the first trimester [10]. Fibroids in a pregnant woman are thought to increase multiple risks such as pain, bleeding, spontaneous miscarriage, preterm labor, preterm premature rupture of membranes (PPROM), placental previa, placental abruption, fetal

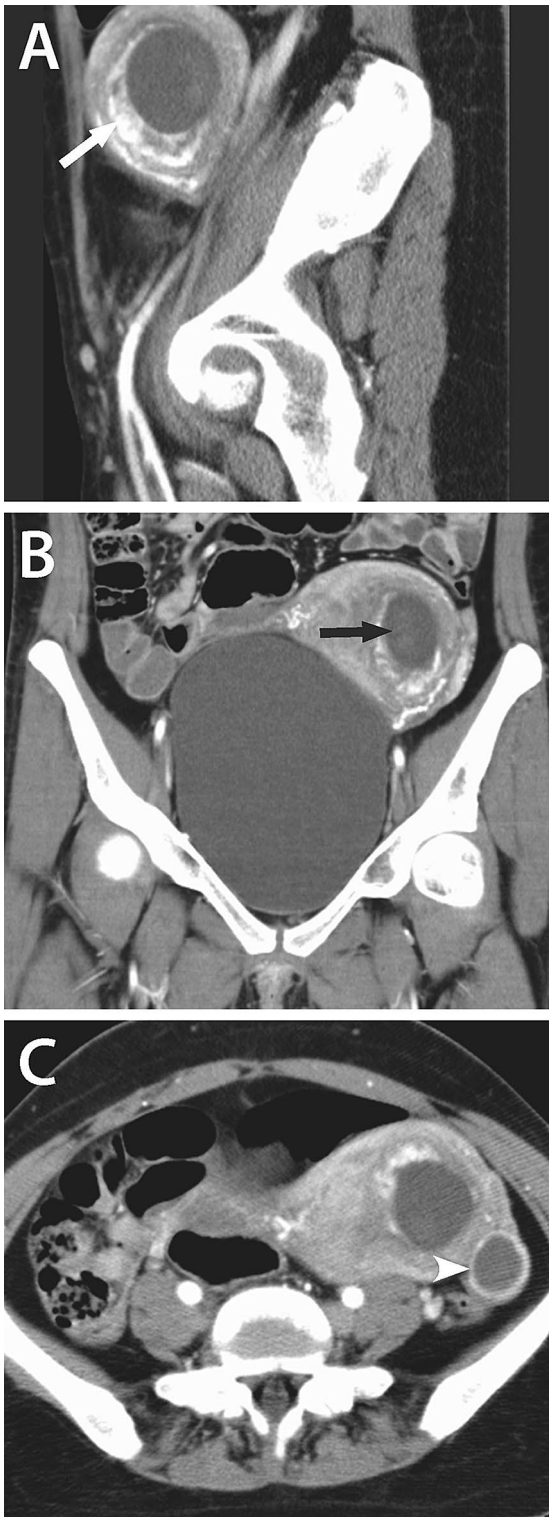

Fig. 3 First trimester pregnancy at estimated gestational age 9 weeks. CT images through the pelvis on a scan performed for maternal trauma showing increased enhancement of the trophoblast (white arrow, **a**), focal increased density within the gestational sac representing the fetal pole (black arrow, **b**), and corpus luteum cyst (white arrowhead, **c**). Fetal outcome was normal

growth restriction, post-partum bleeding, obstructed labor, and malpresentation, making them important to recognize if seen on imaging exams [10, 11]. Leiomyomas can also simulate placental thickening or even hematoma (Fig. 17) [7].

Ectopic pregnancy

In a patient with a positive beta hCG pregnancy test, the most common presentation of ectopic pregnancy is pain and bleeding without an intrauterine pregnancy seen at imaging.

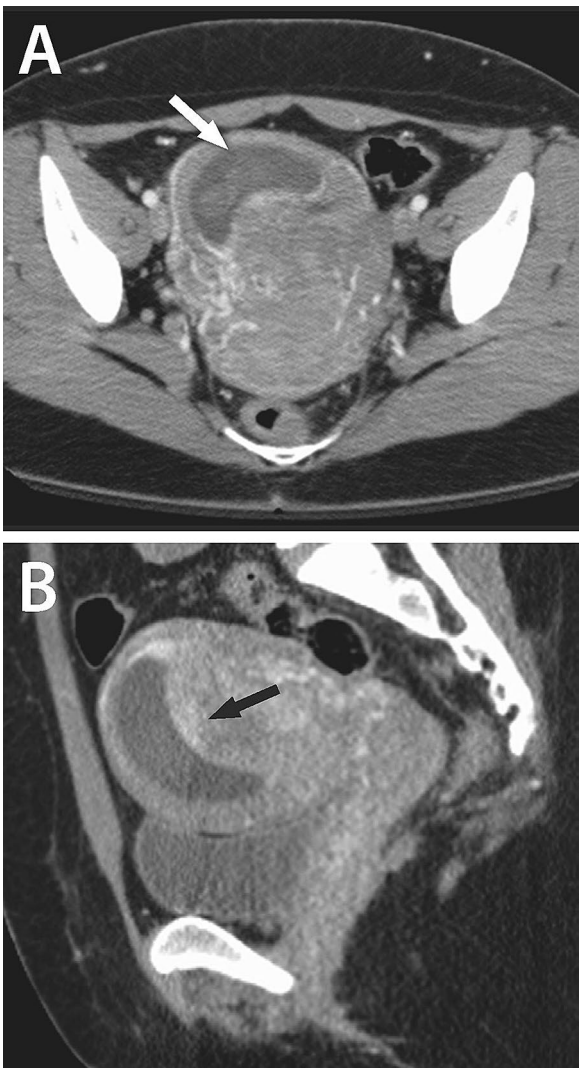

Fig. 4 First trimester pregnancy at estimated gestational age 13 weeks. CT scan performed for maternal trauma showing focal increased density within the gestational sac correlating with the fetus (white arrow, **a**) in addition to increased enhancement of the trophoblast along the posterior wall indicating the location of the placenta (black arrow, **b**). Fetal outcome was normal

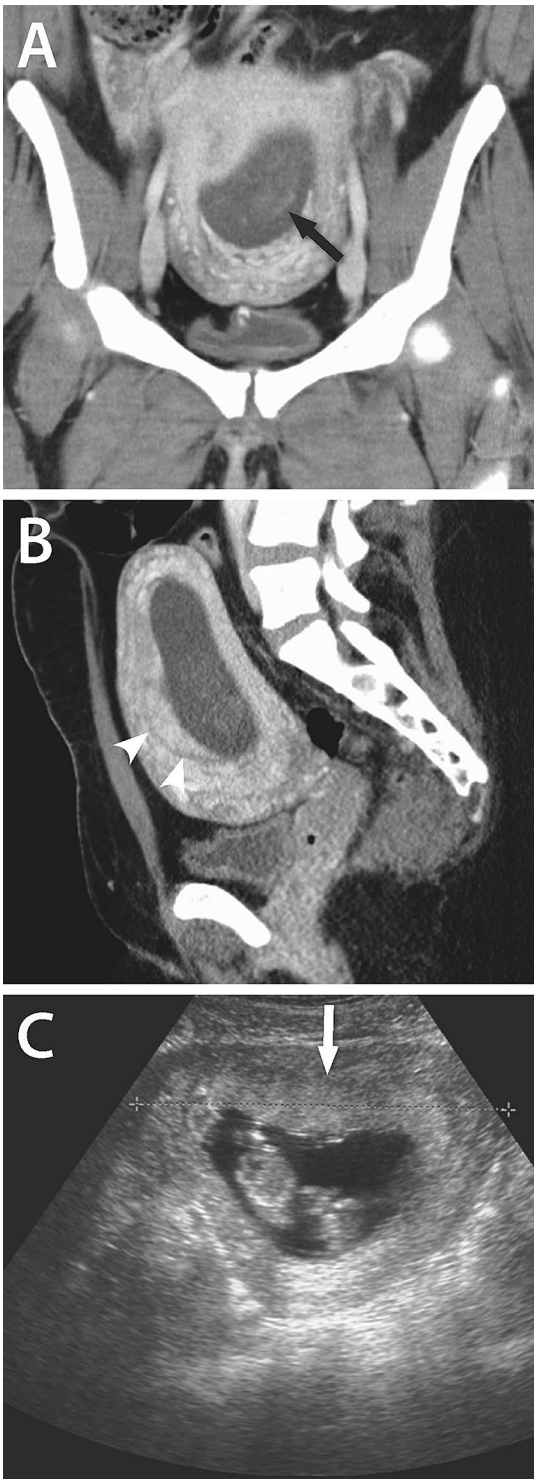

Fig. 5 First trimester pregnancy at estimated gestational age 13 weeks. CT scan performed for maternal trauma showing focal increased density within the gestational sac correlating with the fetus (black arrow, **a**) in addition to a hypodense crescent marking the anterior placental attachment (white arrowheads, **b**) Ultrasound performed 3 days later confirms anterior placental location (white arrow, **c**). Fetal outcome was normal

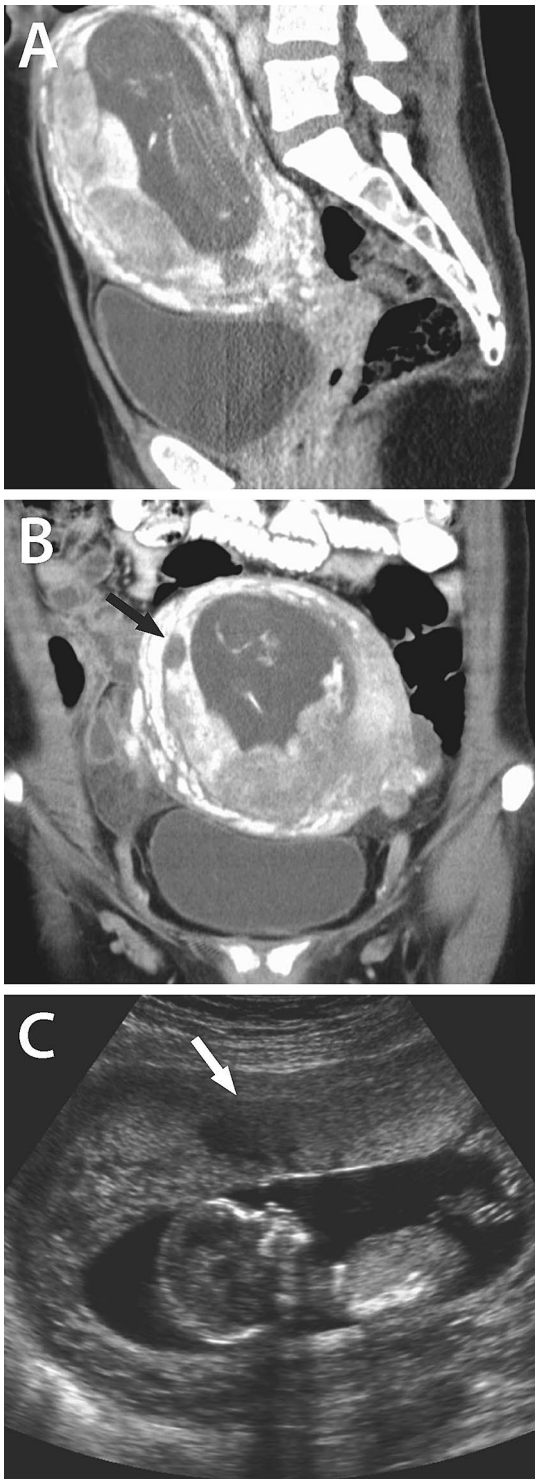

Fig. 6 Second trimester pregnancy at estimated gestational age 14 weeks 3 days. CT scan performed for maternal trauma showing increased mineralization of the skeleton and expected diffuse heterogeneous enhancement of the placenta (**a**, **b**). Focal hypodensity within the placenta (black arrow, **b**) corresponds with hypoechoic sonolucency seen on ultrasound from the same day, most consistent with venous lake (white arrow, **c**). Fetal outcome was normal

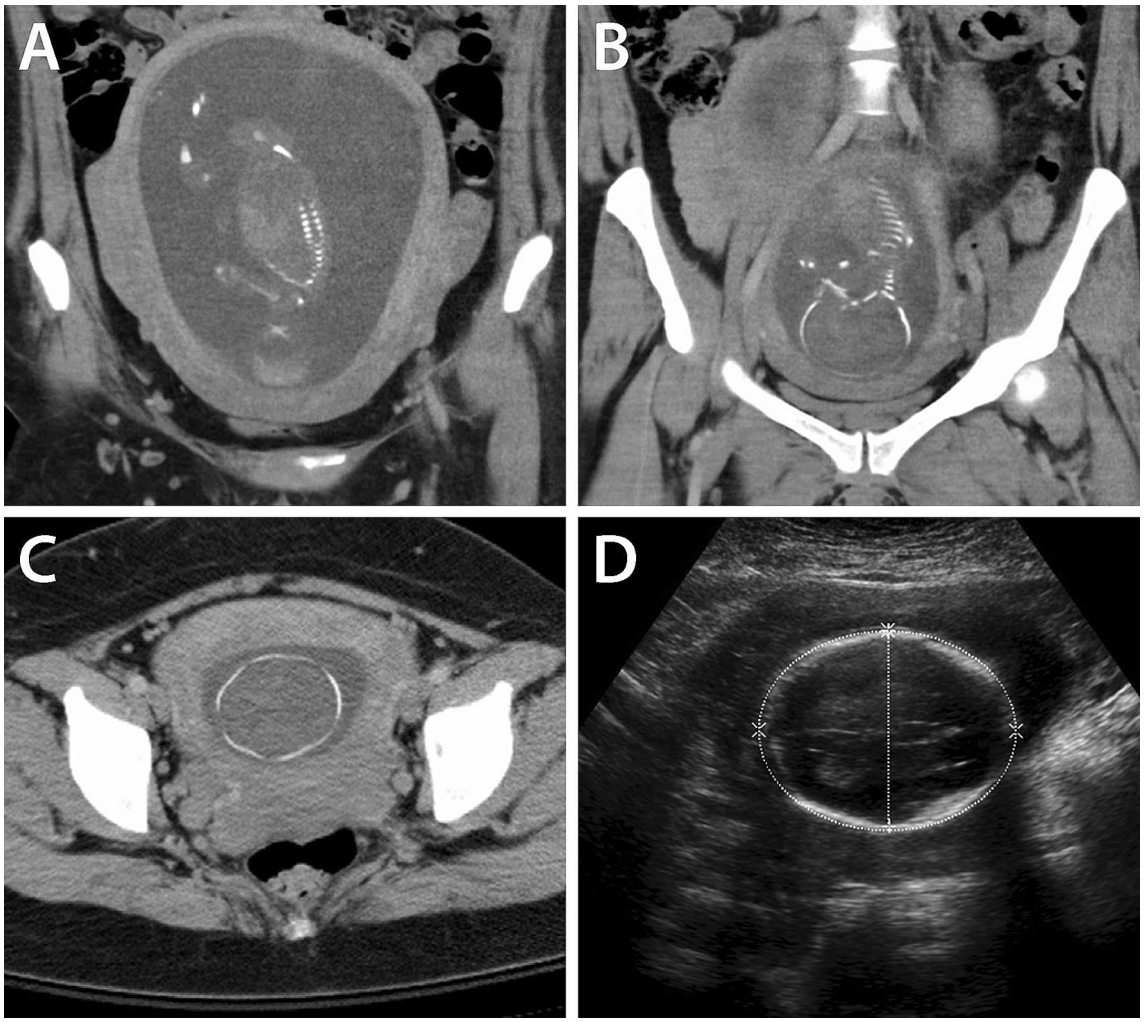

Fig. 7 Second trimester pregnancy at estimated gestational age 16 weeks. CT scan performed for maternal trauma showing increasing mineralization of the fetal skeleton (**a**–**c**). Multiplanar reconstruction can be used to measure the biparietal diameter (BPD) if unknown. BPD was also measured on ultrasound from 2 days earlier (**d**). Fetal outcome was normal

The location is most frequently ampullary or isthmic, but less frequently interstitial, cervical, Cesarean scar, ovarian, and abdominal ectopic pregnancies can occur [12]. On CT, a ruptured tubal ectopic pregnancy most commonly presents with a heterogeneous adnexal mass and hemoperitoneum, potentially with other evidence of early pregnancy as discussed above (Fig. 18) [12, 13].

Ovarian torsion

Pregnant patients are at increased risk of ovarian torsion as the corpus luteal cyst in early pregnancy can be a lead point for torsion. It is estimated that 10% to 20% of adnexal torsions occur in pregnancy [14]. The most common sign of ovarian torsion is enlargement of the ovary and adnexa, with one case series finding torsed ovaries measuring between 4 and 20 cm [15]. Additional CT findings can include an

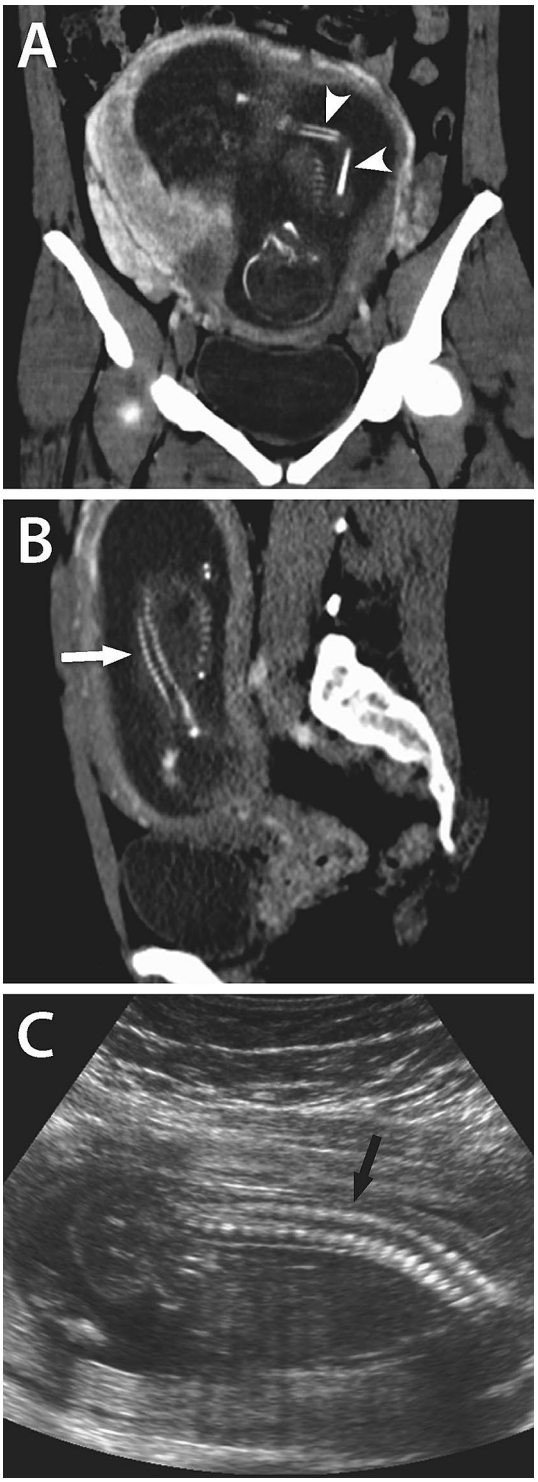

Fig. 8 Second trimester pregnancy at estimated gestational age 18 weeks. CT scan performed for maternal trauma showing mineralization of the humerus, radius, ulna (white arrowheads, **a**), and thoracic spine well demonstrated (white arrow, **b**). Thoracic spine demonstrated on ultrasound 8 days later (black arrow, **c**). Fetal outcome was normal

adnexal mass in the midline, deviation of the uterus to the side of the affected ovary, ascites, a thickened fallopian tube, and decreased central ovarian enhancement (Fig. 19) [16]. Small peripheral ovarian follicles of uniform size seen on ultrasound may not be well seen on CT examination [15]. Vascular flow resulting in enhancement of the ovary does not exclude ovarian torsion and may indicate that the ovary is still viable, particularly if there is central enhancement [17].

Intrauterine device

An intrauterine device can be seen as a dense T-shaped structure within the endometrial cavity (Fig. 20). The presence of an intrauterine device places the patient at increased risk for spontaneous abortion, preterm delivery, and chorioamnionitis [18]. These risks are further increased if the decision is made to retain the device during pregnancy. The current committee opinion of the American College of Obstetricians and Gynecologists states that if the patient is pregnant and the strings are visible, the device should be removed [19]. Visualization of an intrauterine device on CT should prompt evaluation for secondary signs of infection such as infiltration of the periuterine fat or increased free fluid in the pelvis. The presence of an IUD should be particularly mentioned as a potential source of infection if there is a maternal history of fever.

Malignancy

Screening for maternal cervical cancer occurring during pregnancy has a positivity rate similar to that of non-pregnant patients with 5–8% of pap smears abnormal and an incidence of cervical cancer at 1–10 out of 100,000 pregnancies [20]. In patients with a confirmed invasive cervical cancer, ultrasound and/or MRI would be preferred for further staging during pregnancy [21]. However, CT can be used to evaluate for lymphadenopathy, metastases, and hydronephrosis, particularly prior to chemotherapy. The primary tumor may not be well-defined by CT but usually presents as ill-defined enlargement of the cervix (Fig. 21) [22].

Placental abruption

Placental abruption occurs in approximately 1% of all pregnancies [23]. There are multiple traumatic and non-traumatic risk factors with approximately 40% of women with severe trauma diagnosed with placental abruption and 1–5% of women with minor trauma diagnosed with placental abruption [24]. Clinical presentation includes pain,

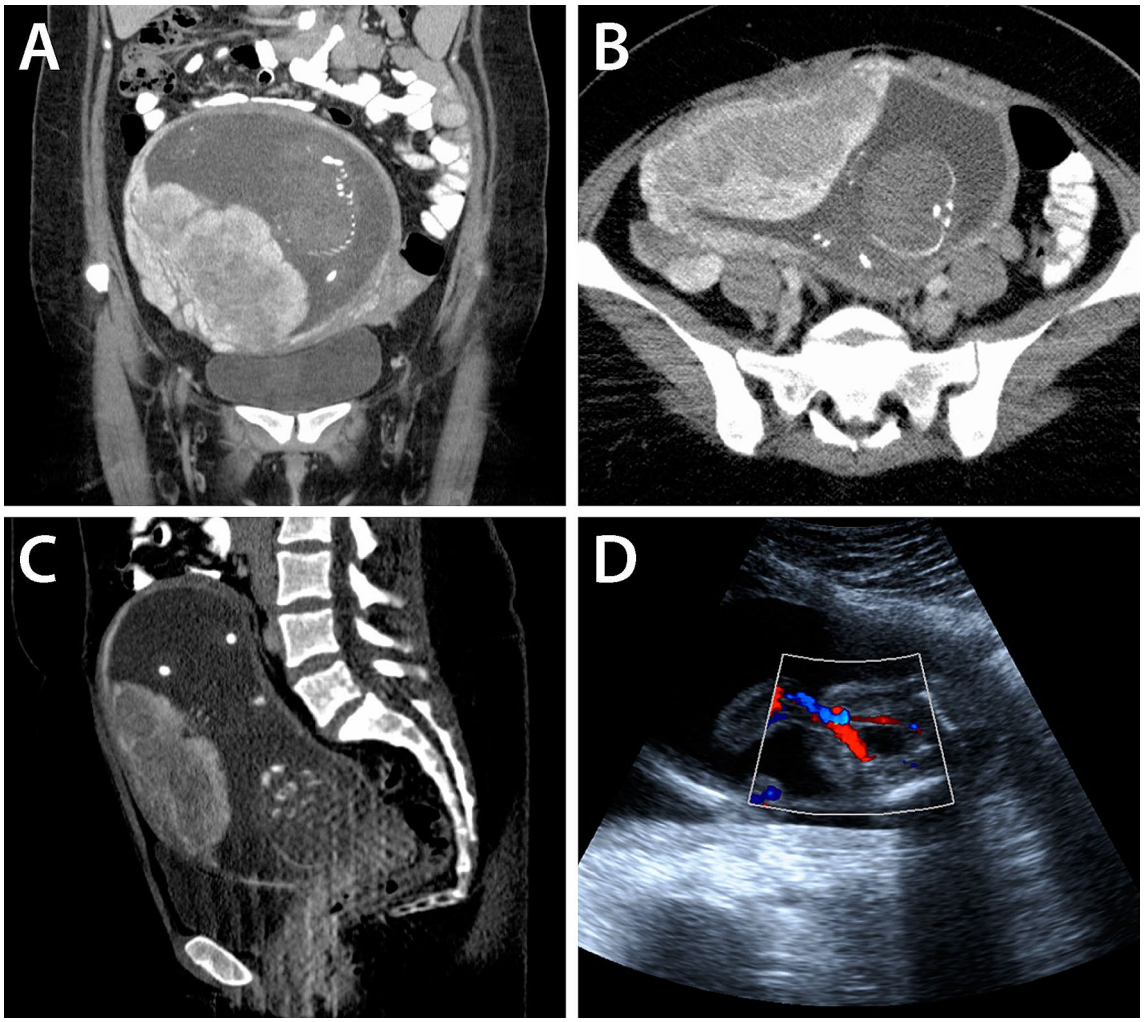

Fig. 9 Second trimester pregnancy at estimated gestational age 21 weeks. CT scan performed for maternal trauma showing thickened placenta (greater than 4 cm) which was likely due to focal myometrial contraction (**a**–**c**), as normal placental thickness was found on ultrasound the same day (not shown). Lack of fetal enhancement (**b**) likely due to bolus timing for maternal injuries as ultrasound performed the same day demonstrated normal flow in the umbilical arteries (**d**). Fetal outcome was normal

bleeding, contractions, and fetal distress. The most likely scenario when CT will be the modality to evaluate placental abruption is in the case of acute abdominal trauma, such as a motor vehicle accident. CT findings of placental abruption include diminished placental enhancement, periplacental hematoma, placental thickening, and separation of the placenta. On the CT trauma imaging evaluation, hematomas can be preplacental, retroplacental, intraplacental, or marginal (Fig. 22). Careful evaluation should be undertaken to identify periplacental hematomas which can be isodense to surrounding placenta and myometrium [6, 7]. As compared to the rounded hypodense areas of slightly decreased enhancement corresponding with the normal cotyledons, areas of abruption tend to be full thickness and form acute

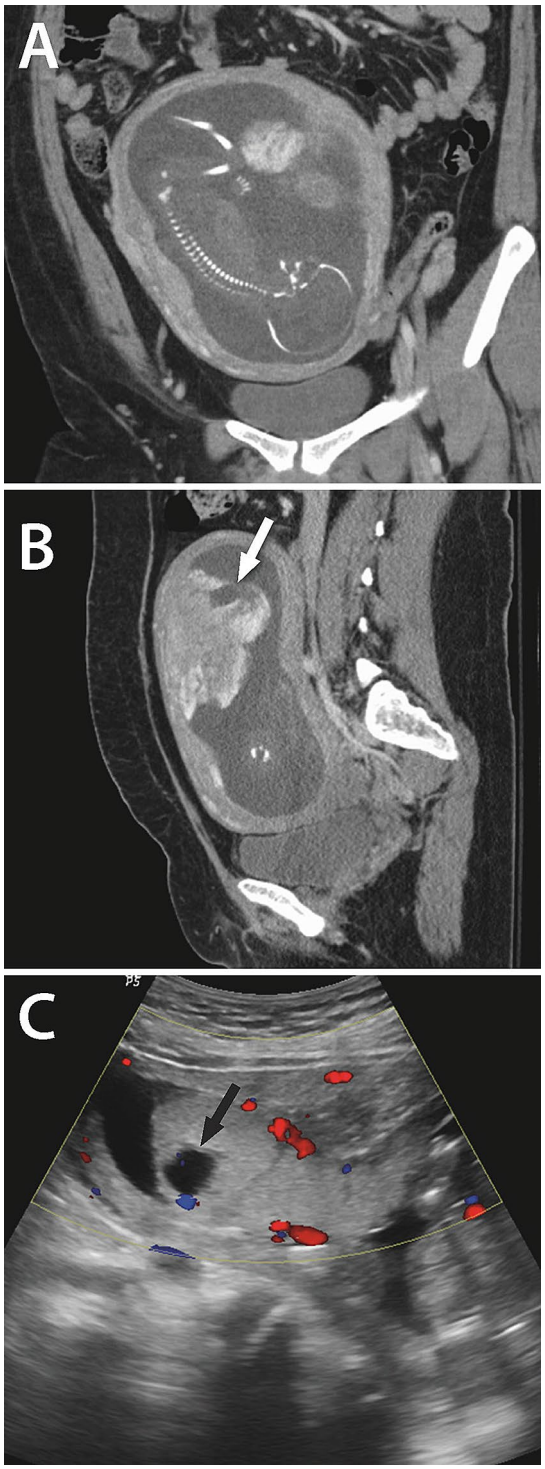

Fig. 10 Third trimester pregnancy at estimated gestational age 28 weeks. CT scan performed for maternal trauma demonstrating mineralization of the fetal skeleton and faint visualization of the internal structures (**a**). Hypodense focus within the placenta (white arrow, **b**) corresponds with sonolucency on ultrasound performed the same day without internal echoes, most consistent with placental cyst (black arrow, **c**). Fetal outcome was normal

angles with the myometrium [25]. A grading scale has been proposed for placental abruption evaluation by CT that differentiates expected hypodensities in the placenta from more concerning areas by shape and location and takes into account the percentage of remaining enhancing placenta, with progressively increasing concern as the percentage of remaining placental enhancement decreases (Figs. 23, 24, 25) [24, 26].

Traumatic injury

CT is the main diagnostic modality to evaluate maternal injury in pregnant patients with major trauma. Trauma is the leading cause of non-obstetrical maternal mortality in pregnancy with the overall incidence of approximately 1 in 12 pregnancies and causes including motor vehicle collision, fall/slip, burn, domestic violence, suicide, homicide, penetrating trauma, and toxic exposure [27]. Fetal loss can occur in 40% to 50% of life-threatening traumas and 1% to 5% of minor traumas [25].

Placental abruption, discussed above, is the most common cause of fetal demise in trauma when the mother survives [25]. Less common causes include uterine rupture, premature rupture of the membranes, and spontaneous abortion. Uterine rupture presents with a full thickness defect in the uterus wall and extrusion of the fetus into the abdomen. Premature rupture of membranes can be suggested by a low amount of amniotic fluid. Spontaneous abortion presents with low lying products of conception, products of conception in the cervix or vagina, or blood in the cervix or vagina [25]. Ongoing clinical care of the mother may demonstrate known fetal demise in various stages of evacuation (Figs. 26, 27). Close investigation of fetal bony structures can identify fracture injuries in some cases (Fig. 28). Care should be taken to not mistake growth plates and skull sutures for fractures. Orthogonal and 3D reconstructions can aid in evaluation.

Conclusion

Abdominal CT is infrequently performed on pregnant patients due to the risks of ionizing radiation to the fetus. When CT is utilized in the setting of pregnancy, it is usually for maternal evaluation and many times for acute, life-threatening indications. While not validated for primary fetal evaluation, CT correlates for some known obstetrical ultrasound findings can be identified despite suboptimal soft

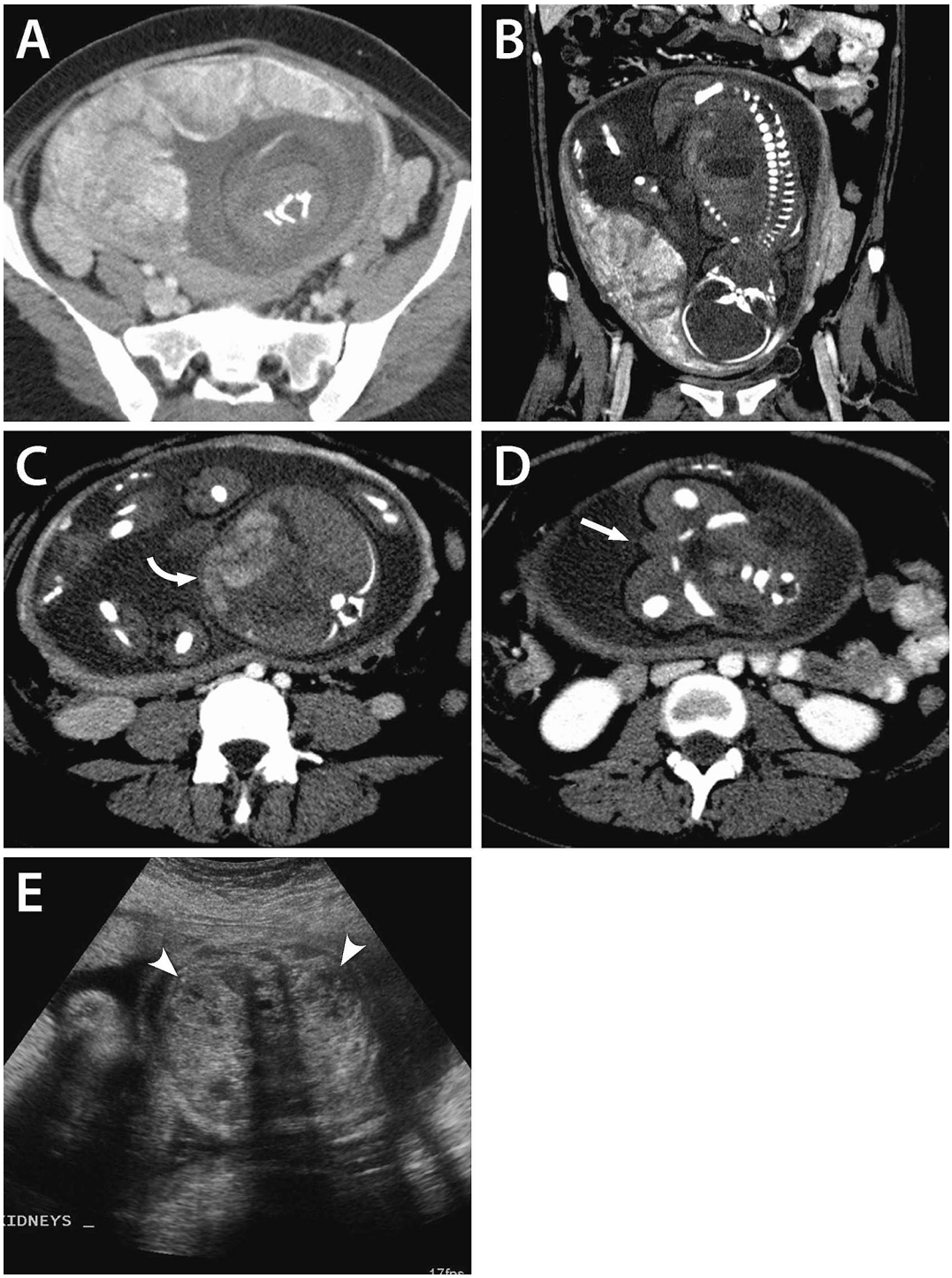

Fig. 11 Third trimester pregnancy at estimated gestational age 31 weeks. CT scan performed for maternal trauma showing rounded cotyledon formation within the placenta (**a**) and visualization of the internal structures including stomach, bladder, liver, and umbilical cord insertion (**b**, **c**). Increased density in fetal small intestine (curved arrow, **c**) of uncertain significance (possibly swallowed blood). Male gender is noted (white arrow, **d**). Ultrasound 1 day earlier demonstrates kidneys which were not well demonstrated on CT (arrowheads, **e**). Fetal outcome was normal

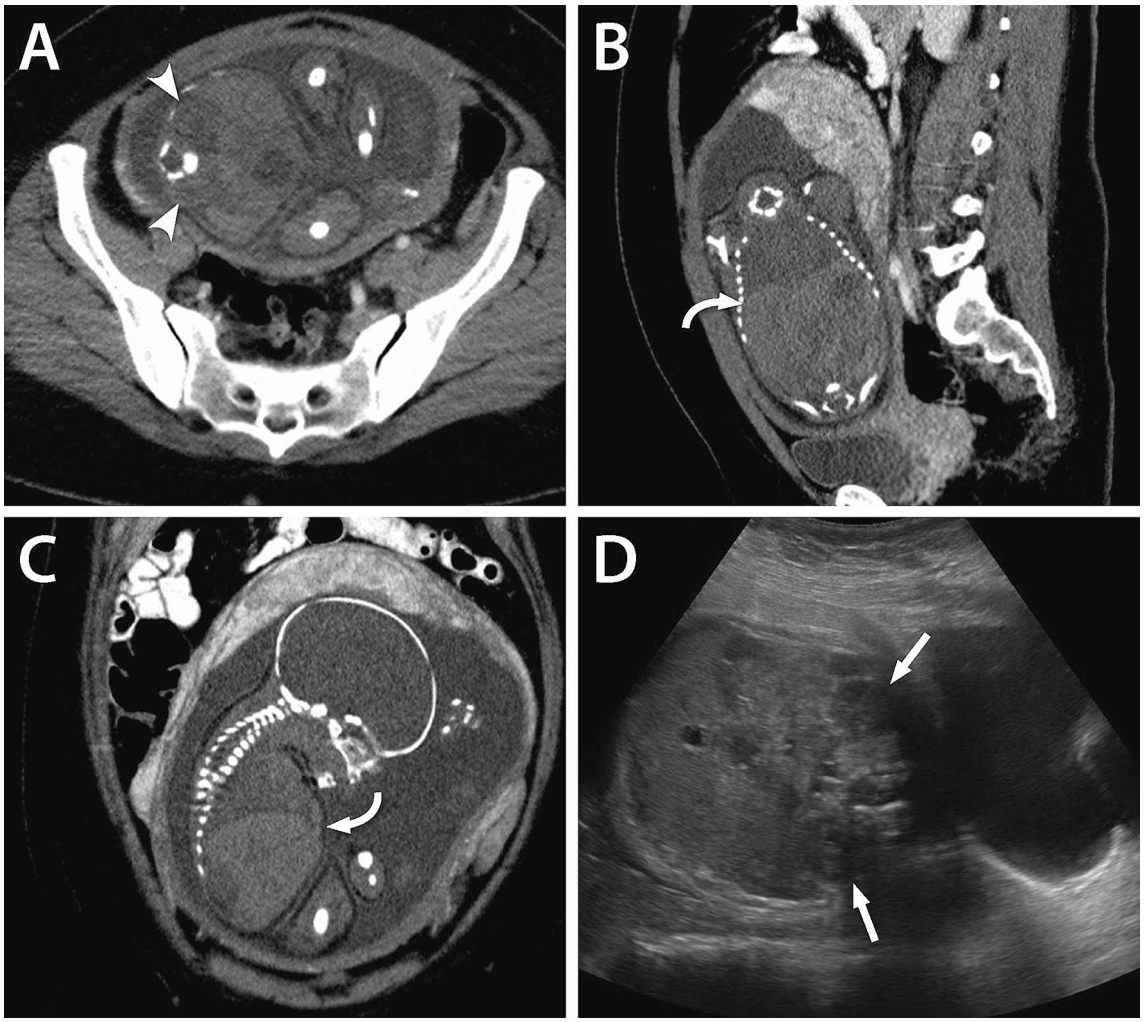

Fig. 12 Third trimester pregnancy at estimated gestational age 33 weeks. CT performed for maternal trauma demonstrating fetal subcutaneous fat separate from surrounding amniotic fluid (**a**–**c**). There is improved CT visualization of fetal kidneys (arrowheads, **a**), with kidneys also shown on comparison ultrasound from the same day (white arrows, **d**). Separation of fluid filled lung and the more dense liver allows visualization of the right hemidiaphragm (curved arrows, **b**, **c**). Fetal outcome was normal

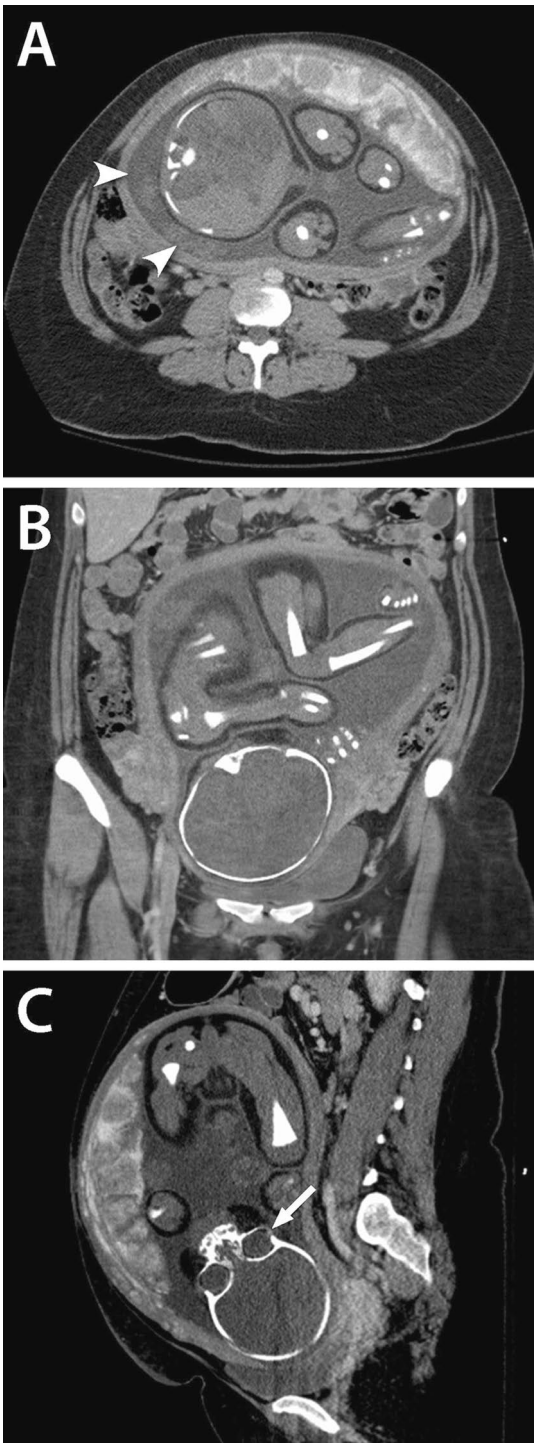

Fig. 13 Third trimester pregnancy at estimated gestational age 39 weeks. CT scan performed for maternal trauma showing hyperdense structure in the amniotic fluid (arrowheads, **a**) corresponding with umbilical cord (not hemorrhage). Rounded structures within the placenta correspond with cotyledons (**a**, **c**). Well-formed skeletal structures, including bony orbit (white arrow, **c**), improved delineation of the subcutaneous fat, kidney, liver, cord insertion, and other internal structures can be seen (**a**–**c**). Fetal outcome was normal

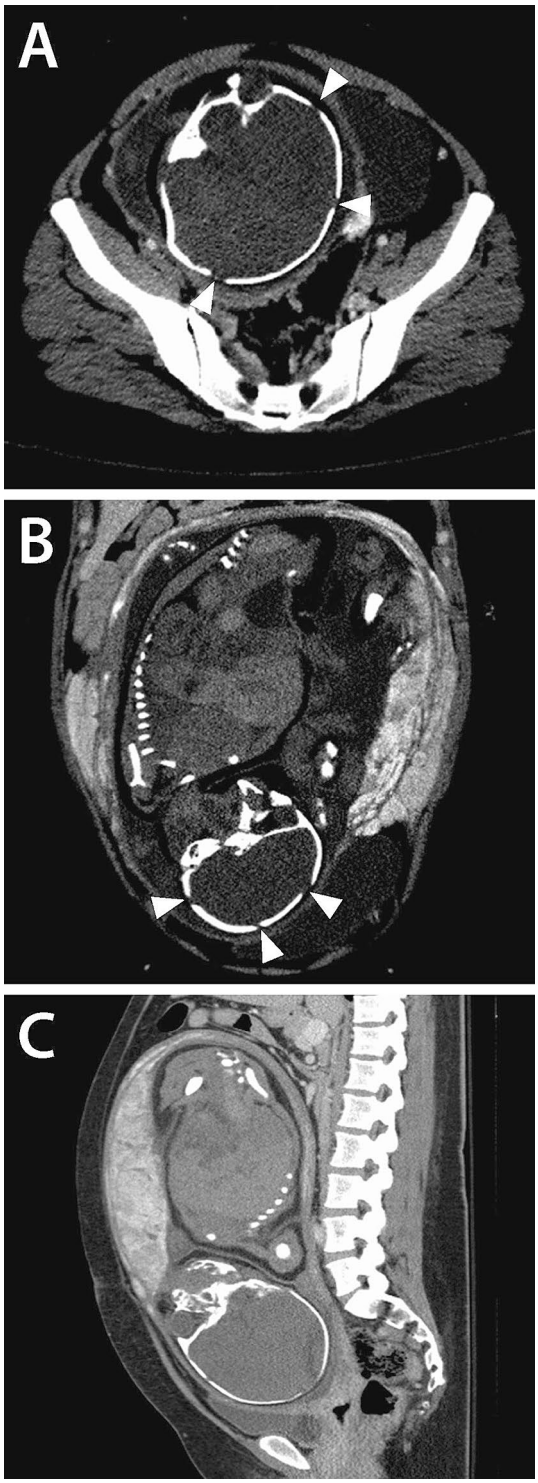

Fig. 14 Third trimester pregnancy at estimated gestational age > 40 weeks. CT scan performed for maternal trauma demonstrating further fetal maturation with skull sutures visualized (arrowheads, **a**, **b**). Placental location, fetal position, biparietal diameter, and maternal pelvic diameter can be evaluated to assist in delivery planning (**a**–**c**). Fetal outcome was normal

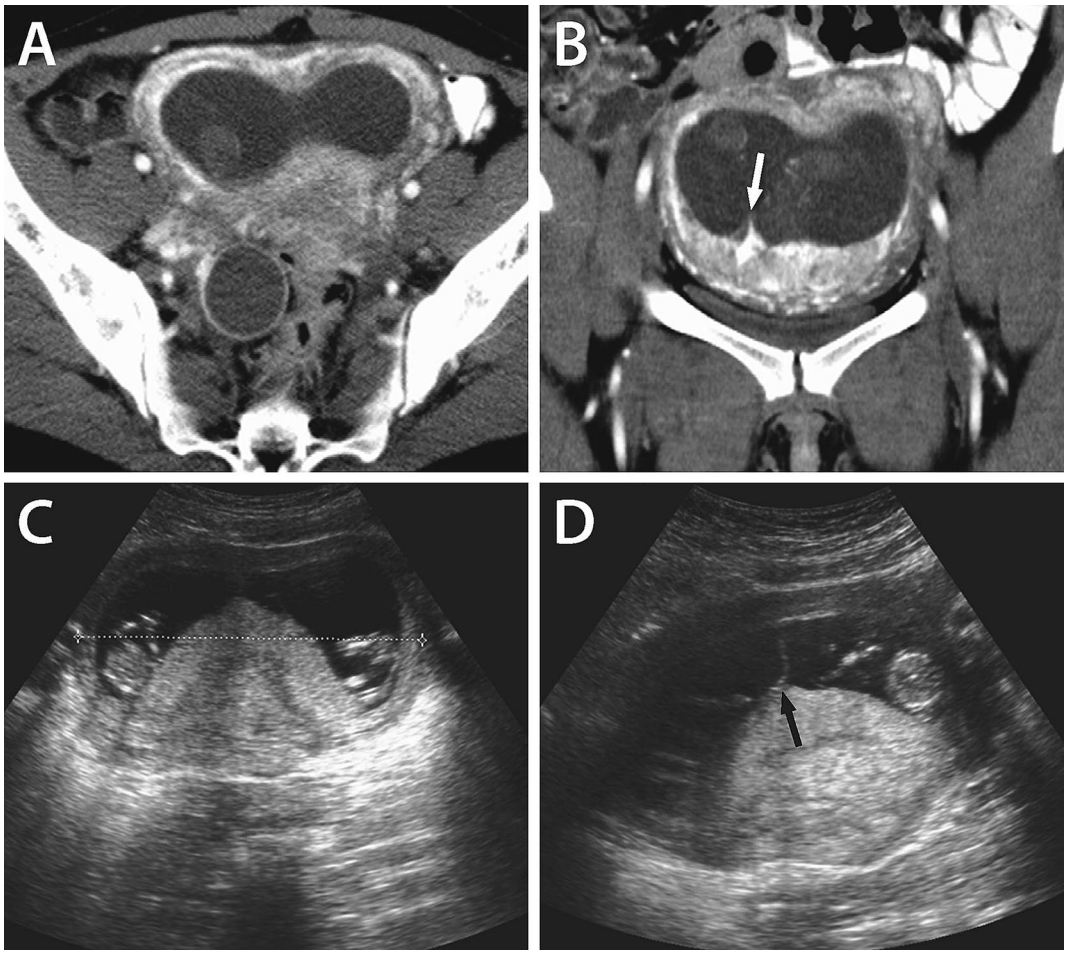

Fig. 15 Multiple gestations. First trimester pregnancy at estimated gestational age 12 weeks. CT scan performed for maternal trauma with ultrasound correlation showing two gestational sacs and faintly hyperdense structures representing two separate fetuses (**a**–**c**). Triangular appearance of the chorion as it invaginates the amniotic membranes (white arrow, **b**) with similar ultrasound appearance (black arrow, **d**) indicating dichorionic diamniotic twin pregnancy. Fetal outcome was normal

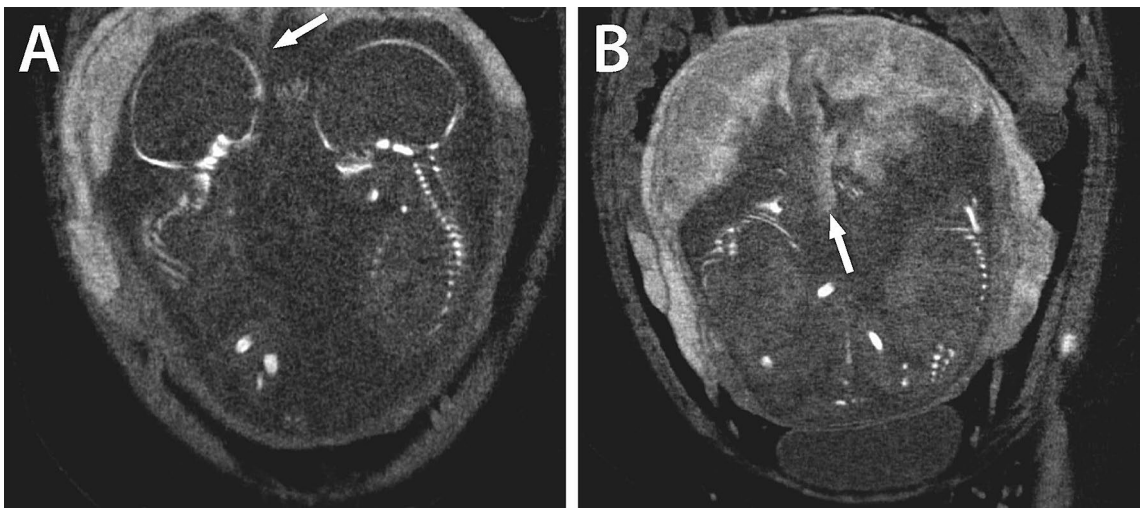

Fig. 16 Multiple gestations. Second trimester pregnancy at estimated gestational age 24 weeks. CT scan performed for maternal trauma showing increased mineralization of the fetal skeletons and triangular appearance of the chorion (white arrows, **a**, **b**) as it invaginates the amniotic membranes indicating dichorionic diamniotic twin pregnancy. Fetal outcome was normal

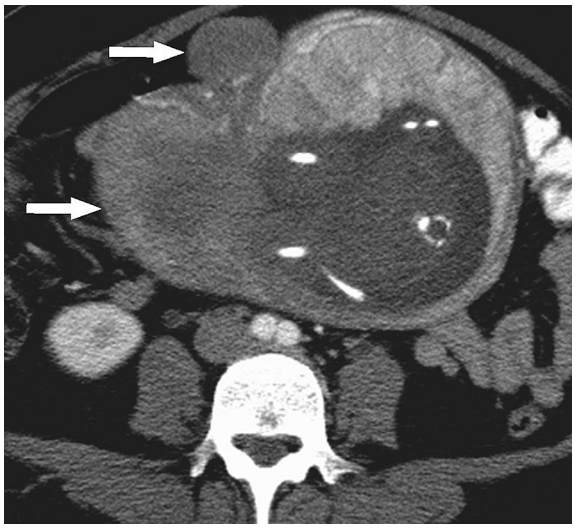

Fig. 17 Uterine fibroid. Second trimester pregnancy at estimated gestational age 22 weeks. CT scan revealing several adjacent subserosal fibroids (white arrows)

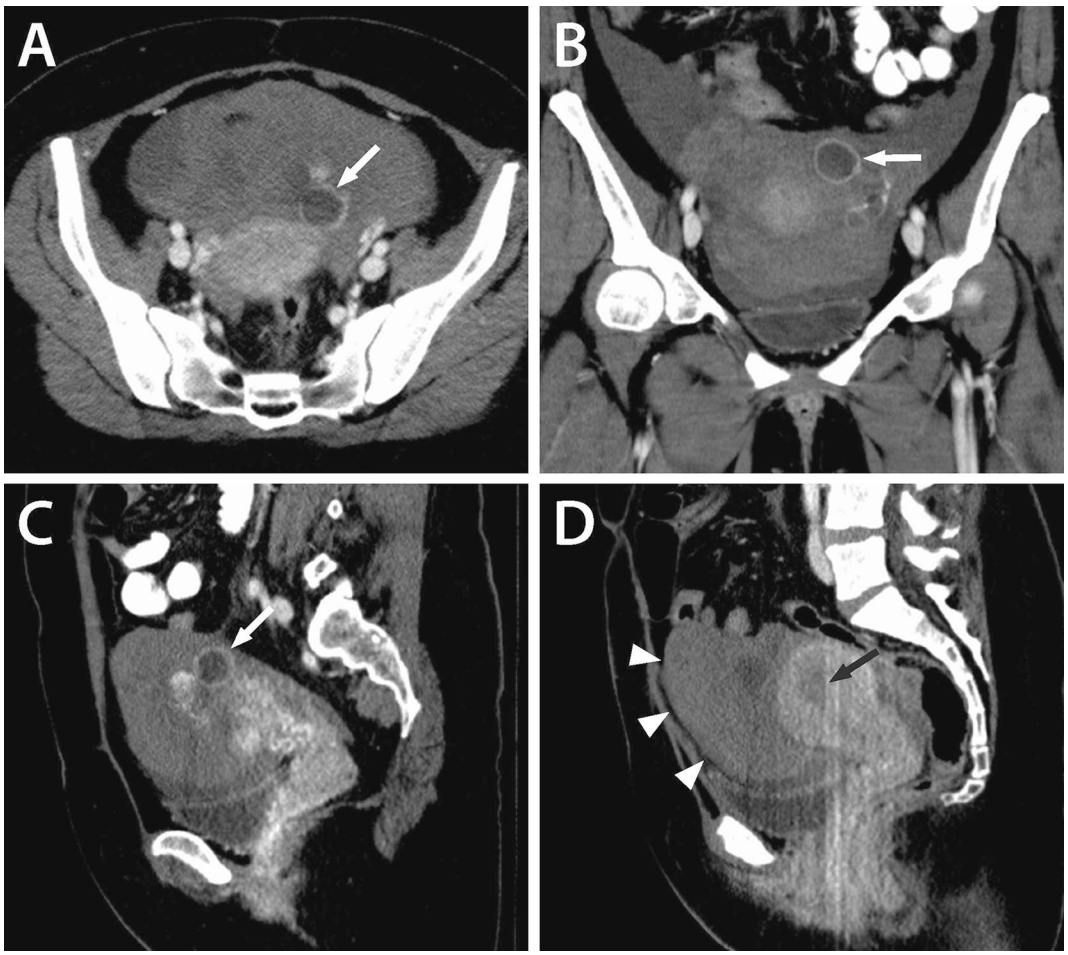

Fig. 18 Ectopic pregnancy. Patient presented with abdominal pain and hemodynamic instability. Emergent CT was performed with subsequent pregnancy test positive. Heterogeneous left adnexal mass with surrounding hemoperitoneum (white arrowheads, **a**–**d**) was identified with possible gestational sac within the left adnexa (white arrows, **a**–**c**). Endometrium was inhomogeneous (black arrow, **d**)

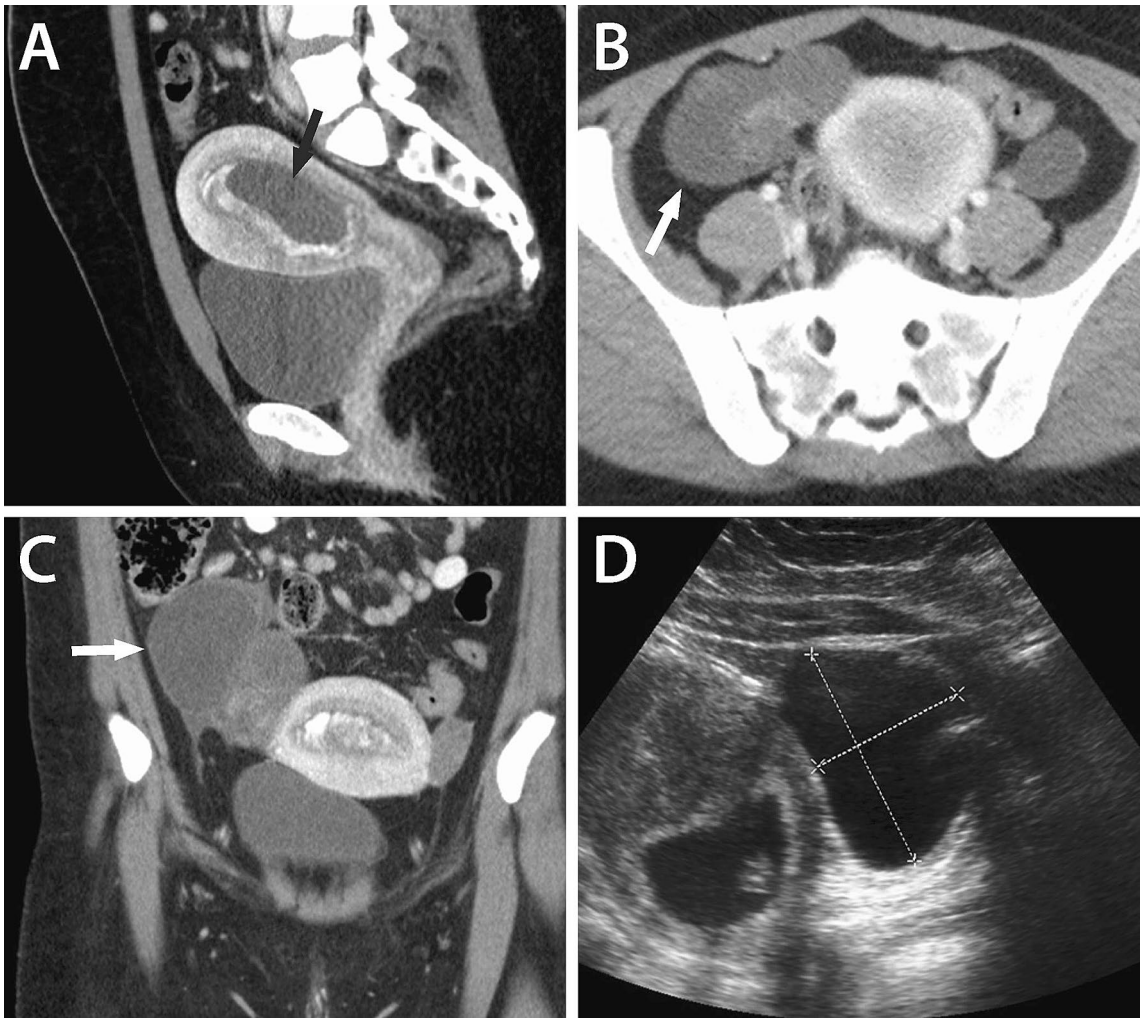

Fig. 19 Ovarian torsion. First trimester pregnancy at estimated gestational age 9 weeks. Patient presented with severe abdominal pain, and CT scan was performed. Amniotic sac is present within the endometrium (black arrow, **a**). Large low density lesion within enlarged right adnexa with surrounding inflammatory changes (white arrows, **b**, **c**). Low density adnexal lesion shown to represent simple appearing cyst on ultrasound (**d**). Patient was taken to the operating room where paratubal cyst was identified, and torsion was confirmed

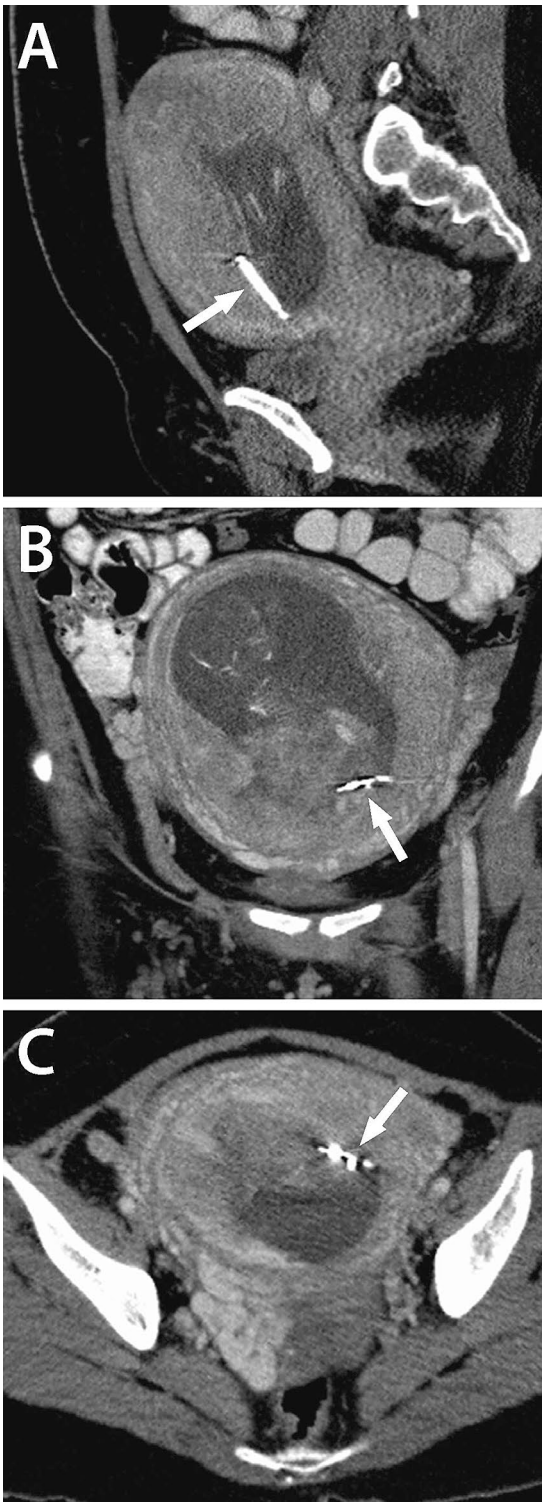

Fig. 20 Intrauterine device. Second trimester pregnancy at estimated gestational age 14–15 weeks. CT scan was performed for maternal fever of unknown origin. Dense T-shaped intrauterine device was present adjacent to the fetus (white arrows, **a**–**c**). Fetal demise occurred 2 days later

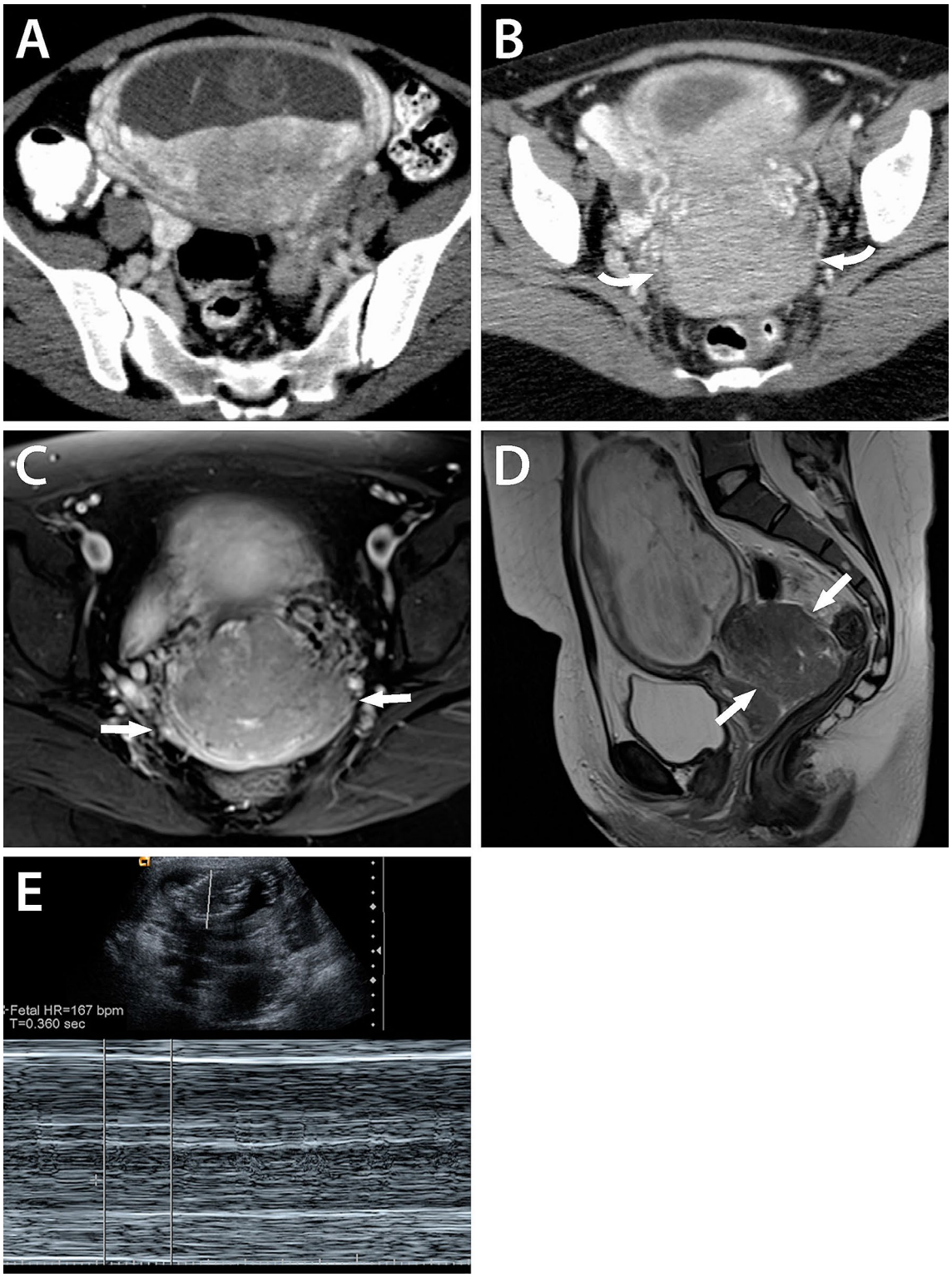

Fig. 21 Cervical cancer. First trimester pregnancy at estimated gestational age 13 weeks. CT images showing gestational sac (**a**) and bulky cervical mass (curved arrows, **b**). MRI images show cervical mass extending to the parametria (white arrows, **c**, **d**). Ultrasound demonstrates viable fetus (**e**)

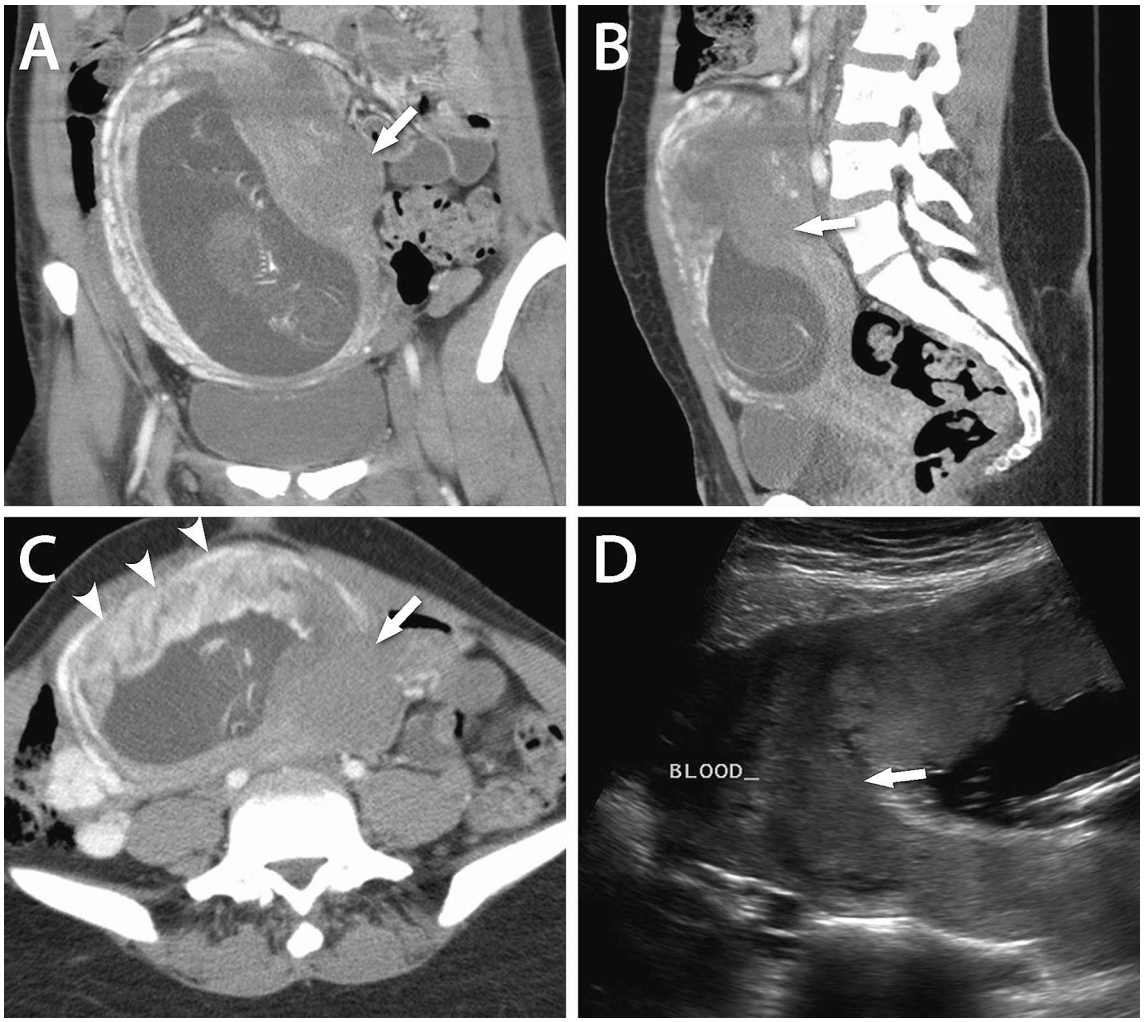

Fig. 22 Placental abruption following trauma. Second trimester pregnancy at estimated gestational age 17 weeks. CT scan and ultrasound showing marginal placental abruption after motor vehicle collision. Subchorionic hematoma extends from below the margin of the placenta (white arrows, **a**–**d**). Otherwise, normal placental enhancement (arrowheads, **c**). Patient was managed conservatively and had a normal term delivery

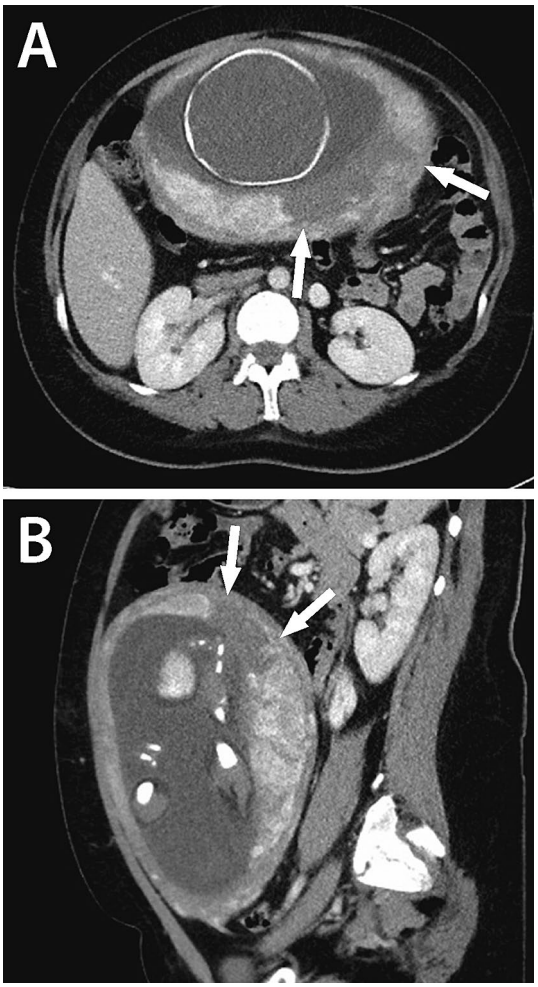

Fig. 23 Placental abruption following trauma. Third trimester pregnancy at estimated gestational age 31 weeks. CT scan performed after motor vehicle collision showing full thickness area of placental hypoenhancement consistent with abruption, estimated at less than 25% of the total placental volume (white arrow, **a**, **b**). Clinical indicators were reassuring and patient was managed conservatively and discharged 3 days later without complications

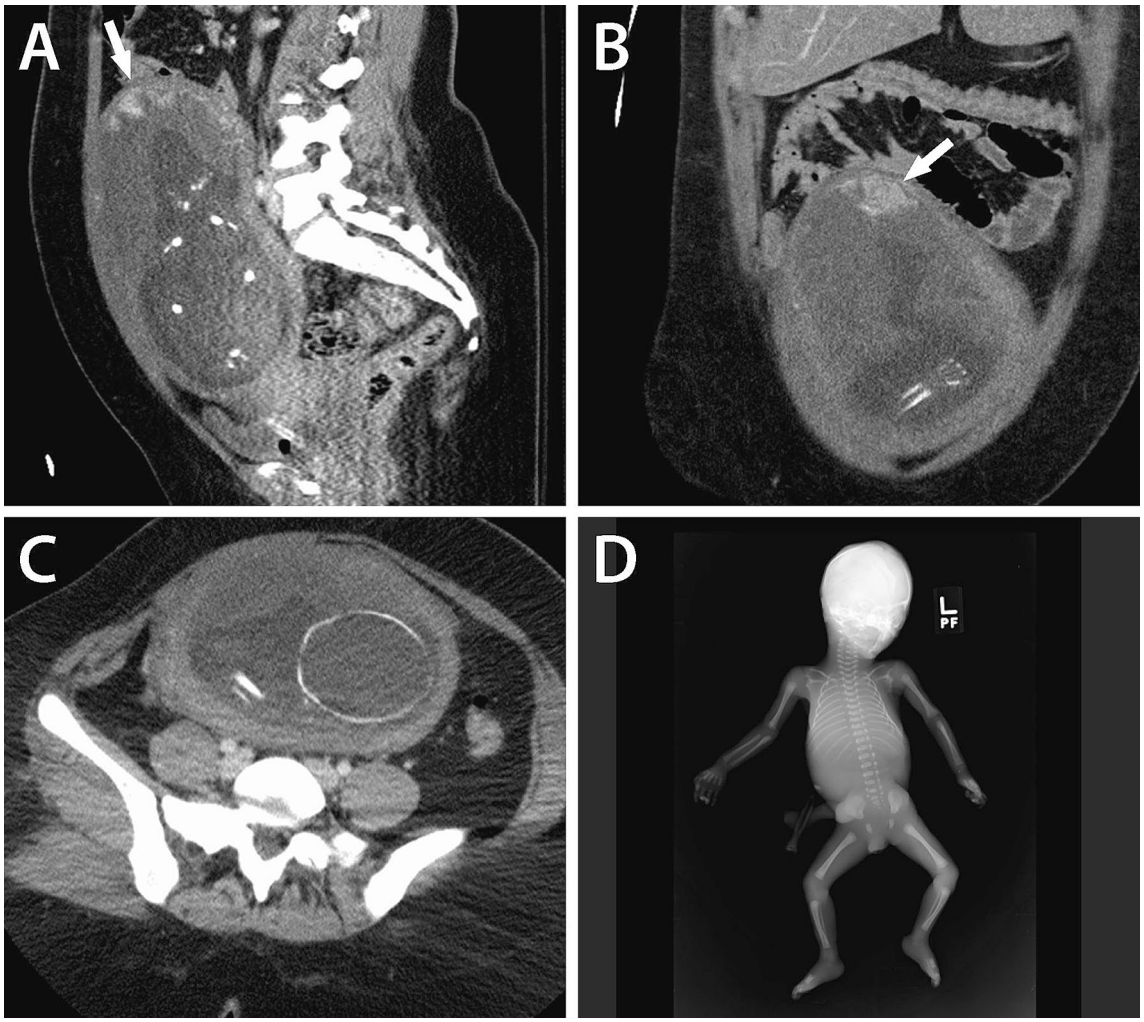

Fig. 24 Placental abruption following trauma. Second trimester pregnancy at estimated gestational age 25 weeks. CT scan performed after motor vehicle collision demonstrating significantly diminished placental enhancement estimated at greater than 50% (**a**–**c**) with only small areas of persistent enhancement (white arrows, **a**, **b**). In utero fetal demise occurred with subsequent delivery the next day. Fetalgram demonstrates no visible fetal abnormalities (**d**)

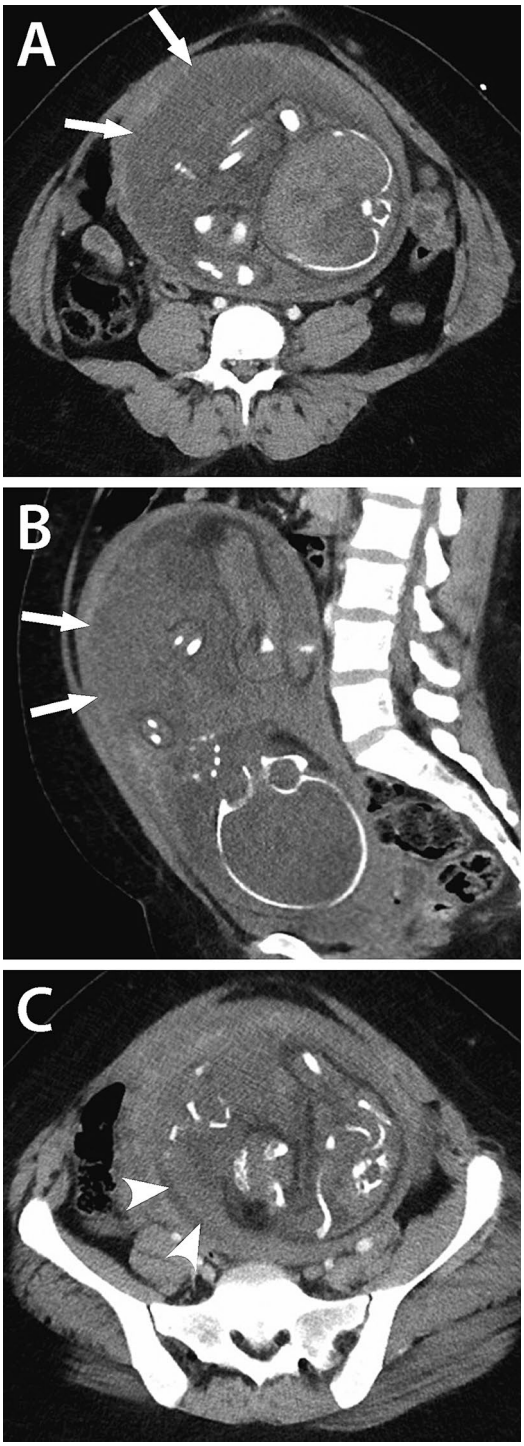

Fig. 25 Placental abruption following trauma. Third trimester pregnancy at estimated gestational age 32 weeks. CT scan performed after motor vehicle collision showing hypoenhancement of the entire placenta consistent with abruption (white arrows, **a**, **b**). Hyperdense material is demonstrated throughout the amniotic sac consistent with hemorrhage (arrowheads, **c**). Lack of cardiac motion was discovered with bedside ultrasound (not shown) consistent with fetal demise. Delivery occurred immediately thereafter with confirmation of placental abruption

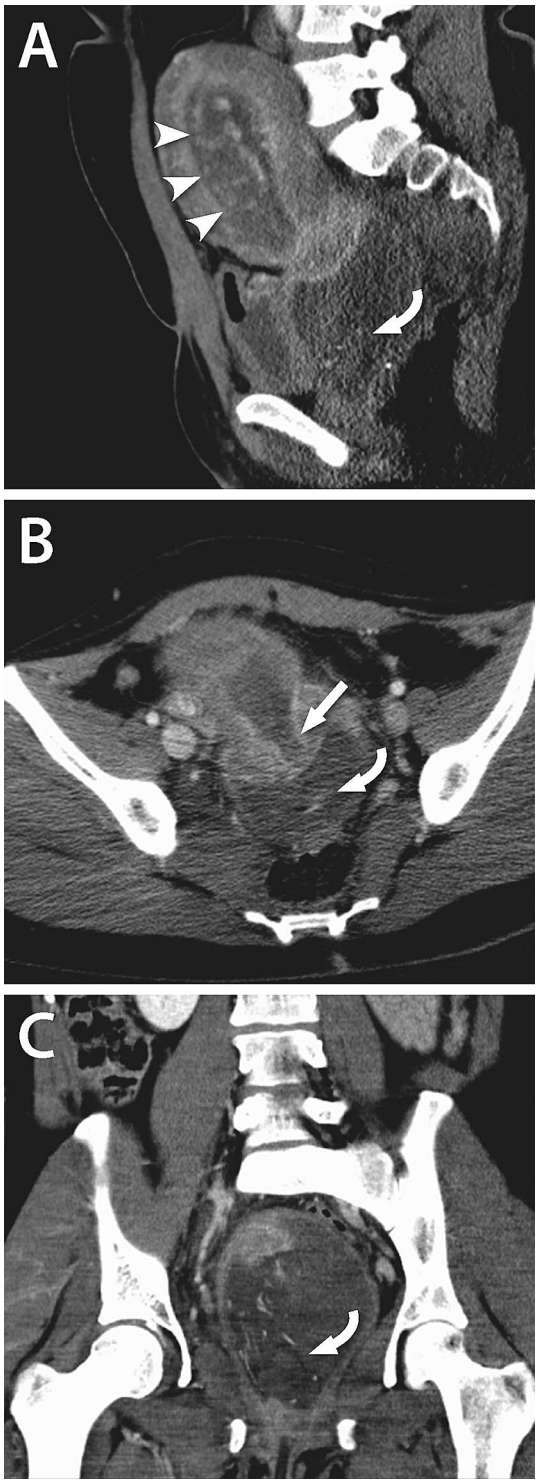

Fig. 26 Intrauterine fetal demise with spontaneous abortion following trauma. Second trimester pregnancy at estimated gestational age 14 weeks. CT scan performed for maternal trauma demonstrating hypoenhancement of the placenta (arrowheads, **a**), open cervix (white arrow, **b**), and products of conception in the vaginal canal (curved arrow, **b**, **c**)

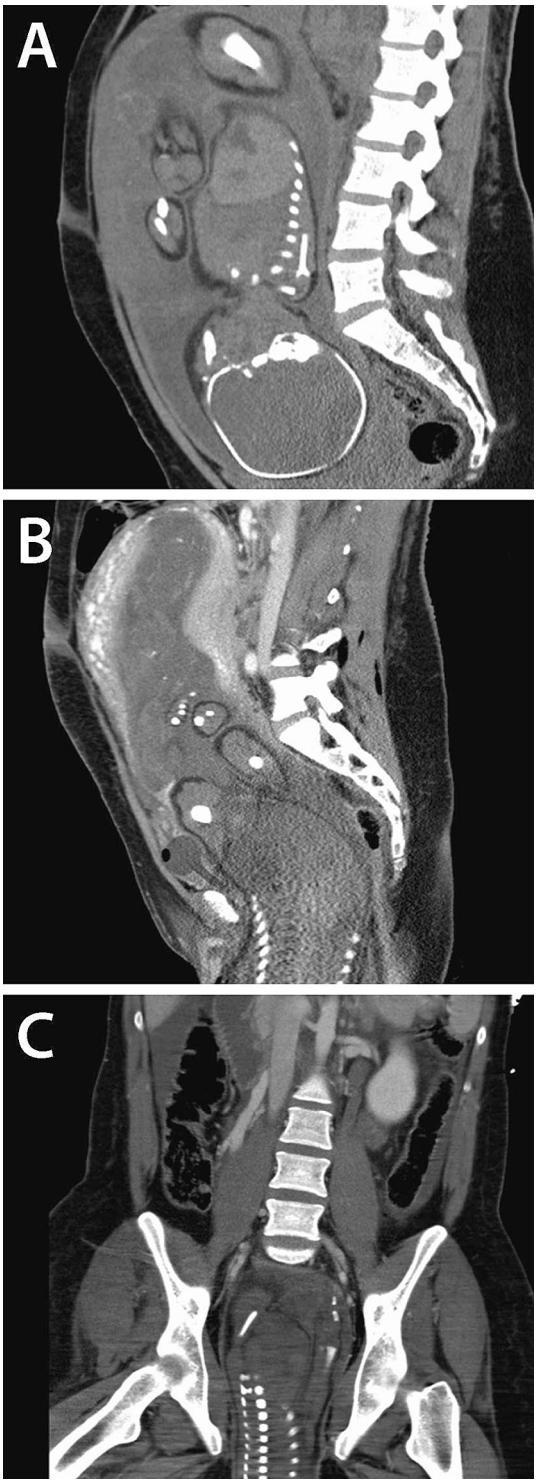

Fig. 27 Intrauterine fetal demise with spontaneous abortion following trauma. Third trimester pregnancy at estimated gestational age 31 weeks. CT scan performed for maternal trauma (without IV contrast due to IV malfunction) showing no definite fetal abnormalities identified (**a**). Repeat CT performed with IV contrast 8 h later demonstrates passage of fetal parts into the vaginal canal (**b**, **c**)

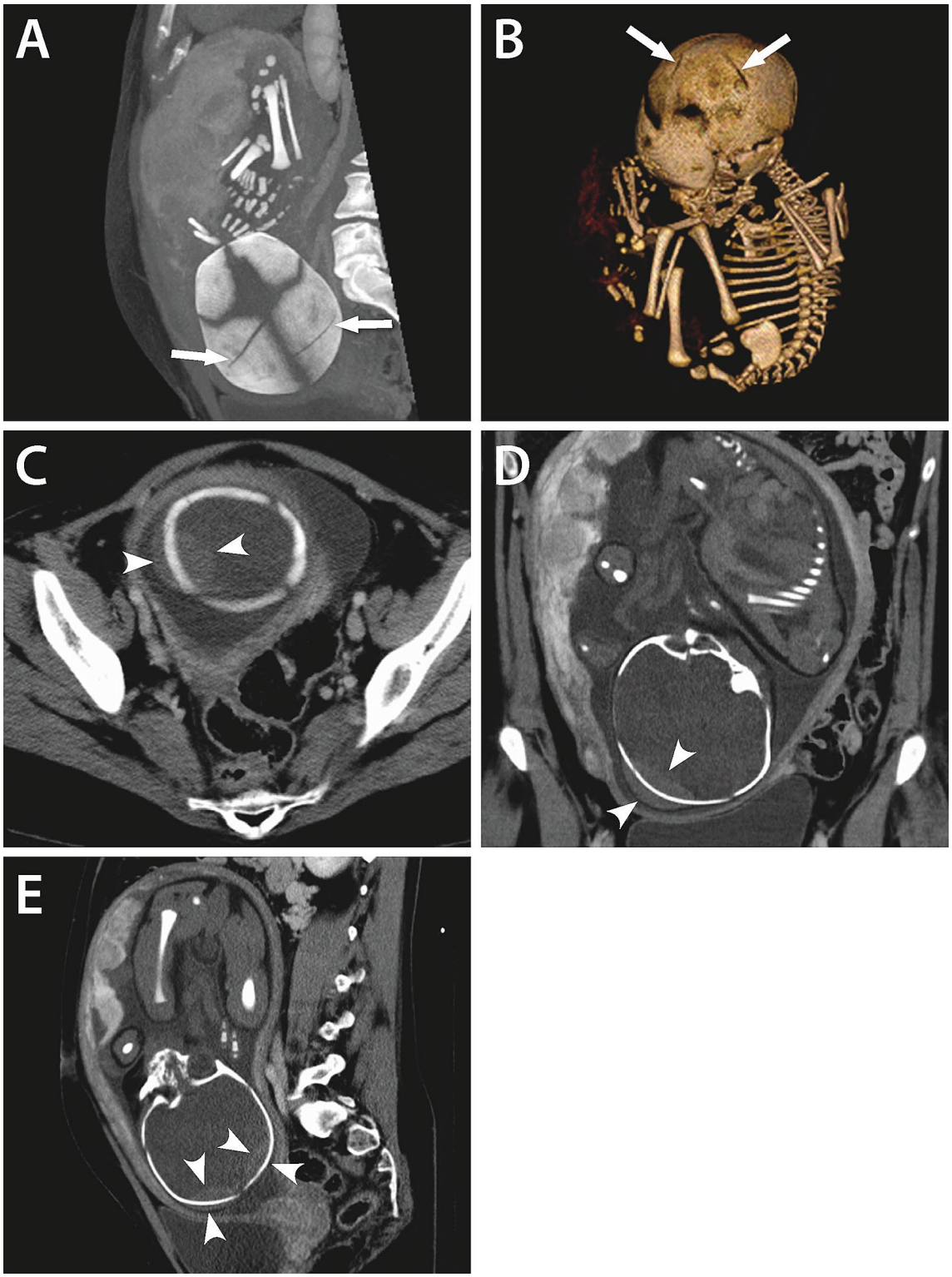

Fig. 28 Fetal trauma. Third trimester pregnancy at estimated gestational age 35–36 weeks. CT scan performed for maternal trauma with MIP image and 3D reconstruction demonstrating asymmetric oblique linear lucencies in the skull which are narrower than skull sutures consistent with fetal skull fractures (white arrows, **a**, **b**). Adjacent scalp swelling and bilateral epidural hematomas (arrowheads, **c**–**e**) are shown. Patient underwent emergent Cesarean section with confirmed neonatal head injury, Apgar scores 9/9, and eventual normal hospital discharge

tissue contrast compared to ultrasound and MRI. Evaluation of the pregnancy on the CT scan obtained for other indications can yield important information which may expedite and better triage maternal and fetal care.

References

1. Lazarus E, Mayo-Smith WW, Mainiero MB, Spencer PK (2007) CT in the evaluation of nontraumatic abdominal pain in pregnant women. Radiology 244 (3):784-790. https://doi.org/10.1148/radiol.2443061634
2. Jain C (2019) ACOG Committee Opinion No. 723: Guidelines for Diagnostic Imaging During Pregnancy and Lactation. Obstet Gynecol 133 (1):186. https://doi.org/10.1097/aog.0000000000003049
3. ACR-SPR practice parameter for imaging pregnant or potentially pregnant adolescents and women with ionizing radiation (2018). American College of Radiology and the Society for Pediatric Radiology Resolution 39
4. Shin DS, Poder L, Courtier J, Naeger DM, Westphalen AC, Coakley FV (2011) CT and MRI of early intrauterine pregnancy. AJR Am J Roentgenol 196 (2):325-330. https://doi.org/10.2214/ajr.09.3723
5. Rodgers SK, Chang C, DeBardeleben JT, Horrow MM (2015) Normal and Abnormal US Findings in Early First-Trimester Pregnancy: Review of the Society of Radiologists in Ultrasound 2012 Consensus Panel Recommendations. Radiographics 35 (7):2135-2148. https://doi.org/10.1148/rg.2015150092
6. Wei SH, Helmy M, Cohen AJ (2009) CT evaluation of placental abruption in pregnant trauma patients. Emerg Radiol 16 (5):365-373. https://doi.org/10.1007/s10140-009-0804-z
7. Fadl S, Moshiri M, Fligner CL, Katz DS, Dighe M (2017) Placental Imaging: Normal Appearance with Review of Pathologic Findings. Radiographics 37 (3):979-998. https://doi.org/10.1148/rg.2017160155
8. Elsayes KM, Trout AT, Friedkin AM, Liu PS, Bude RO, Platt JF, Menias CO (2009) Imaging of the placenta: a multimodality pictorial review. Radiographics 29 (5):1371-1391. https://doi.org/10.1148/rg.295085242
9. Chauhan SP, Scardo JA, Hayes E, Abuhamad AZ, Berghella V (2010) Twins: prevalence, problems, and preterm births. Am J Obstet Gynecol 203 (4):305-315. https://doi.org/10.1016/j.ajog.2010.04.031
10. Lee HJ, Norwitz ER, Shaw J (2010) Contemporary management of fibroids in pregnancy. Rev Obstet Gynecol 3 (1):20-27
11. Cooper NP, Okolo S (2005) Fibroids in pregnancy–common but poorly understood. Obstet Gynecol Surv 60 (2):132-138
12. Febronio EM, Rosas GdQ, Cardia PP, D'Ippolito G (2012) Ectopic pregnancy: pictorial essay focusing on computed tomography and magnetic resonance imaging findings. Radiologia Brasileira 45:279-282
13. Kao LY, Scheinfeld MH, Chernyak V, Rozenblit AM, Oh S, Dym RJ (2014) Beyond ultrasound: CT and MRI of ectopic pregnancy. AJR Am J Roentgenol 202 (4):904-911. https://doi.org/10.2214/ajr.13.10644
14. Born C, Wirth S, Stabler A, Reiser M (2004) Diagnosis of adnexal torsion in the third trimester of pregnancy: a case report. Abdom Imaging 29 (1):123-127. https://doi.org/10.1007/s00261-003-0079-x
15. Hiller N, Appelbaum L, Simanovsky N, Lev-Sagi A, Aharoni D, Sella T (2007) CT features of adnexal torsion. AJR Am J Roentgenol 189 (1):124-129. https://doi.org/10.2214/ajr.06.0073
16. Chang HC, Bhatt S, Dogra VS (2008) Pearls and pitfalls in diagnosis of ovarian torsion. Radiographics 28 (5):1355-1368. https://doi.org/10.1148/rg.285075130
17. Duigenan S, Oliva E, Lee SI (2012) Ovarian torsion: diagnostic features on CT and MRI with pathologic correlation. AJR Am J Roentgenol 198 (2):W122-131. https://doi.org/10.2214/ajr.10.7293
18. Moshos E, Twickler D (2011) Intrauterine devices in early pregnancy: findings on ultrasound and clinical outcomes. American Journal of Obstetrics & Gynecology 204:427.e421-426
19. Committee Opinion No 672 Summary Clinical Challenges of Long-Acting Reversible Contraceptive Methods (2016). Obstet Gynecol 128 (3):674-675. https://doi.org/10.1097/aog.0000000000001637
20. Van Calsteren K, Vergote I, Amant F (2005) Cervical neoplasia during pregnancy: diagnosis, management and prognosis. Best Pract Res Clin Obstet Gynaecol 19 (4):611-630. https://doi.org/10.1016/j.bpobgyn.2005.03.002
21. Hunter MI, Tewari K, Monk BJ (2008) Cervical neoplasia in pregnancy. Part 2: current treatment of invasive disease. Am J Obstet Gynecol 199 (1):10-18. https://doi.org/10.1016/j.ajog.2007.12.011
22. Pannu HK, Corl FM, Fishman EK (2001) CT evaluation of cervical cancer: spectrum of disease. Radiographics 21 (5):1155-1168. https://doi.org/10.1148/radiographics.21.5.g01se311155
23. Oyelese Y, Ananth C (2006) Placental Abruption. Obstetrics and gynecology 108:1005-1016. https://doi.org/10.1097/01.aog.0000239439.04364.9a
24. Manriquez M, Srinivas G, Bollepalli S, Britt L, Drachman D (2010) Is computed tomography a reliable diagnostic modality in detecting placental injuries in the setting of acute trauma? Am J Obstet Gynecol 202 (6):611 e611-615. https://doi.org/10.1016/j.ajog.2010.01.027
25. Raptis CA, Mellnick VM, Raptis DA, Kitchin D, Fowler KJ, Lubner M, Bhalla S, Menias CO (2014) Imaging of trauma in the pregnant patient. Radiographics 34 (3):748-763. https://doi.org/10.1148/rg.343135090
26. Saphier NB, Kopelman TR (2014) Traumatic Abruptio Placenta Scale (TAPS): a proposed grading system of computed tomography evaluation of placental abruption in the trauma patient. Emerg Radiol 21 (1):17-22. https://doi.org/10.1007/s10140-013-1155-3
27. Mendez-Figueroa H, Dahlke JD, Vrees RA, Rouse DJ (2013) Trauma in pregnancy: an updated systematic review. Am J Obstet Gynecol 209 (1):1-10. https://doi.org/10.1016/j.ajog.2013.01.021